Chapter 10
The Application of CALPHAD Methods

10.1. INTRODUCTION

The purpose of this chapter is to describe the current state of the art for what can be achieved in terms of CALPHAD calculations. It will start with a brief history on how CALPHAD calculations have been used in the past and then concentrate on the complex multi-component materials that can be treated by the software packages described in the previous chapter on computational methods. It will also concentrate on calculations for 'real' materials, which are mainly multi-component and, where possible, comparisons will be made with experimental observations. Little time will, therefore, be spent on binary and ternary calculations, although these can be quite complex and have their own points of interest. There are now so many such calculations that it would be impossible to cover the full range here. Also they must now be considered rather as building blocks for use in calculations which are multi-component in nature. For more extended information the reader is therefore pointed to the 20-year index of the CALPHAD journal (*CALPHAD* 1997) where calculations of binary and ternary systems are regularly published. Some examples of calculated binary and ternary diagrams are shown in Figs 10.1 and 10.2. They show the formation of non-stoichiometric binary and ternary compounds, order–disorder transformations (β/B2 in Ti–Al–Nb), ionic liquids with miscibility gaps, multiple sub-lattice phases, spinel phases, etc., and help demonstrate the state of the art which can now be achieved.

It is possible to separate calculations made under the CALPHAD umbrella into a number of strands. One major area is concerned with substance databases where, with the general exception of the gas phase, phases are modelled as stoichiometric. The problems associated with Gibbs energy minimisation are simpler for such calculations, but they can often involve much larger numbers of phases than would be considered in a multi-component alloy. Alloys probably still account for the majority of CALPHAD publications, as a review of the CALPHAD journal shows a preponderance of papers in this area. This relates back to the development of solution databases, which are more complex in nature than substance databases, and also to the intrinsic early problems of CALPHAD associated with factors such as lattice stabilities and development of new models for metallic systems. The development of models for ionic systems is also another significant, and growing area, sharing much in common with the principles driving the development of alloy

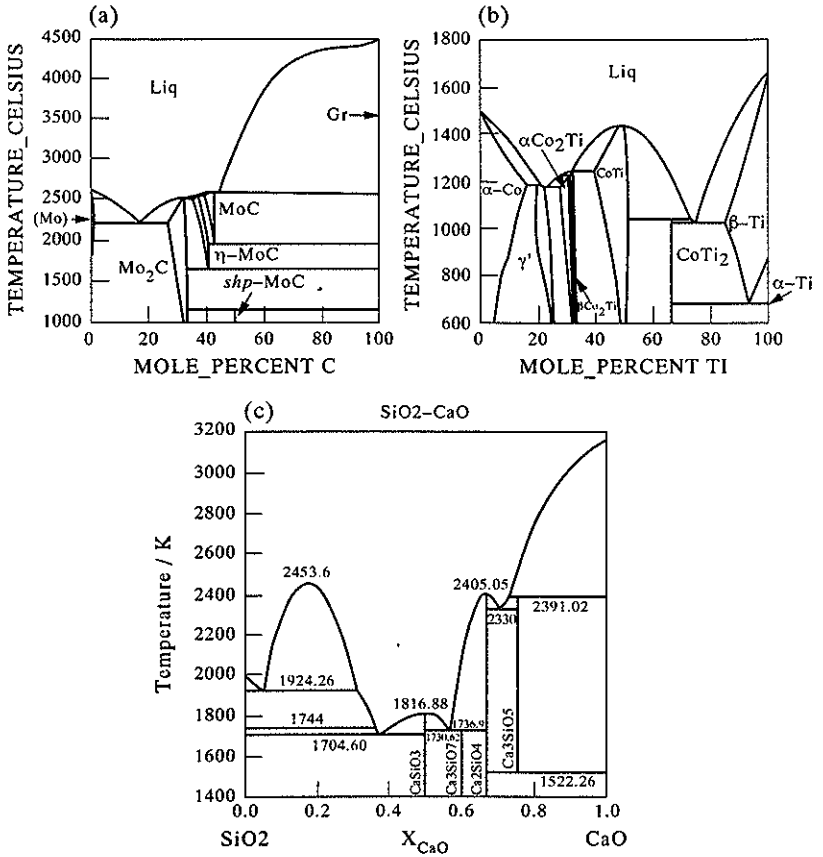

Figure 10.1 Calculated binary phase diagrams for (a) Mo–C (Andersson 1988), (b) Co–Ti (Saunders 1996c) and (c) $CaO–SiO_2$ (Taylor and Dinsdale 1990).

calculations. In ionic systems the aim is to develop models which represent both the mixing properties of ionic substances as well as allowing these to be combined with substance and alloy databases. At present most CALPHAD software packages include models which deal with aqueous solutions, but their general usage has not been great, which is also true for organic systems.

10.2. EARLY CALPHAD APPLICATIONS

Broadly speaking, the first application of CALPHAD methods was intrinsically coupled to experimental thermodynamic or phase-diagram measurements. For

References are listed on pp. 402–408.

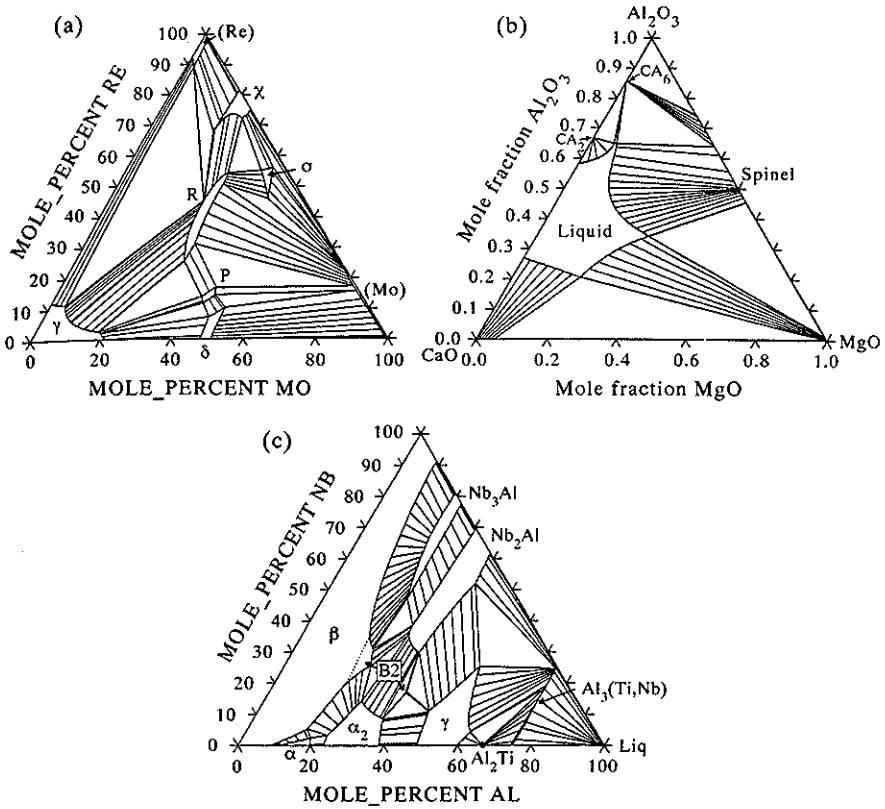

Figure 10.2 Calculated ternary isothermal sections for (a) Ni–Mo–Re at 1000°C (Saunders 1997c), (b) CaO–MgO–Al2O3 at 2000 K (Hallstedt 1992) and (c) isothermal section of Ti–Al–Nb at 1000°C (Saunders 1996a).

example, early work by Kaufman and Clougherty (1964) on Ti–O both explored aspects of modelling as well as coupling of their calculations to experimentally determined O activities. In Europe a number of groups, particularly some of the founder-members of the Scientific Group Thermodata Europe (SGTE), were strongly interested in systems of interest to Fe-based alloys, and work by Counsell *et al.* (1972) on Fe–Ni–(Cu, Cr), by Harvig *et al.* (1972) on Fe–X–C systems and Ansara and Rand (1980) on Fe–Cr–Ni–C clearly demonstrates the concept of coupling of a CALPHAD calculation with experimental determination of phase boundaries and thermodynamics.

An example of an early paper on a binary system is the work of Spencer and Putland (1973) on Fe–V. This combined a review of the thermodynamics and phase diagram of the Fe–V system with new, selective experimental thermodynamic

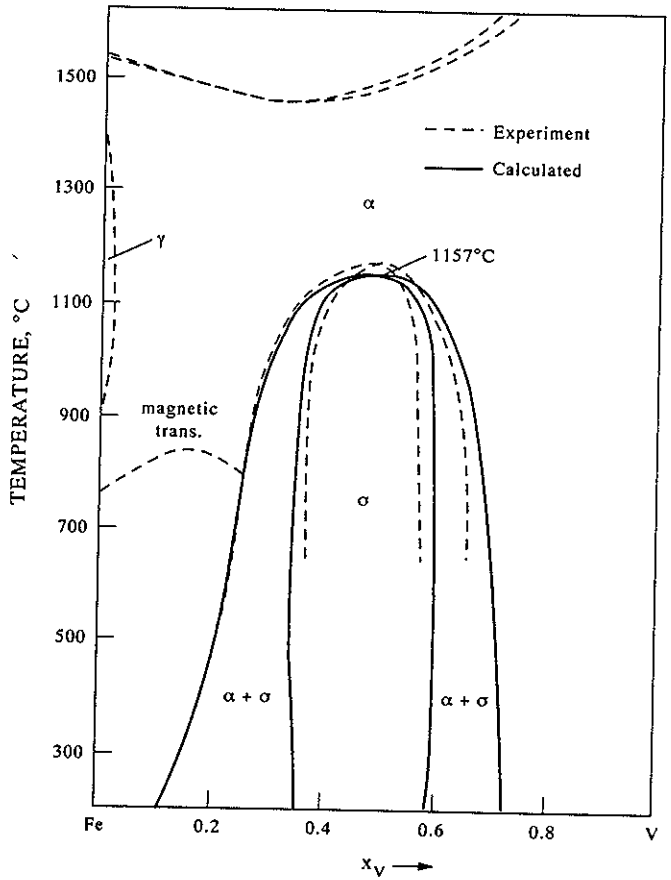

Figure 10.3 Calculated $\alpha+\sigma$ phase boundary for Fe–V with experimental boundaries superimposed.

measurements in order to provide a thermodynamic assessment of the α/σ-phase boundary in this system. Figure 10.3 shows a diagram calculated with their parameters and compares this with the experimentally determined phase diagram. Since then, new assessments have been made for this system, but apart from changes in models and the inclusion of the liquid and γ phases (which are in themselves important developments) the form of the calculated diagram in the region of interest to Spencer and Putland (1973), as well as the calculated thermodynamic properties, have not essentially changed.

In ternary alloys, coupling thermodynamic calculation with experimental work is often essential and a good example of such work is found in the assessment of Cr–Fe–W by Gustafsson (1988). Figure 10.4 shows a calculated isothermal section

References are listed on pp. 402–408.

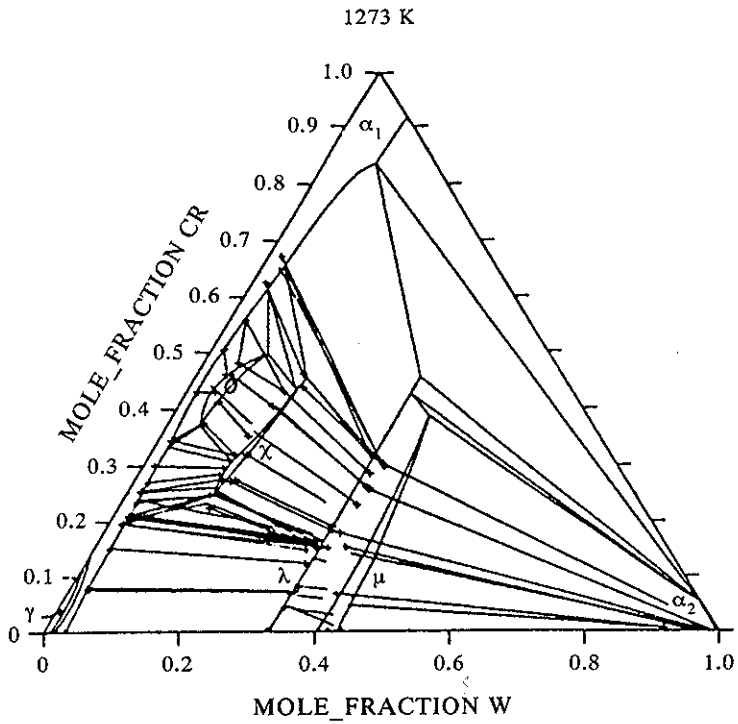

Figure 10.4 Calculated isothermal section of the Cr–Fe–W system with experimental tie-lines superimposed (Gustafson 1988).

at 1273 K which is compared with wide-ranging tie-line experiments carried out by the same author. Ideally, it is helpful to have new experimental backing for assessment work but enough information may exist so that a good assessment can be made with data already available in the literature. Increasingly, the latter situation is becoming the more usual route to providing ternary assessments but, in the authors' opinion, if high-quality results are needed, and there are discrepancies between various literature references, highly accurate experimentation on a small scale is a worthwhile undertaking. An example of such an approach is that undertaken by Yang *et al.* (1992a, b) for the Ni–Al–Ti system, where a few alloys in the $\beta/\beta'/\gamma'$ ternary phase field were all that was necessary to accurately fix this particular phase equilibrium, which was crucial to the development of a new type of intermetallic alloy. The concept of a detailed optimisation of thermodynamic parameters, although initially slower in generating large quantities of data, has eventually led to the ability to make highly accurate calculations in higher-order systems.

The development of models and concepts was also of major importance in the

development of CALPHAD techniques, particularly when dealing with the so-called 'lattice stability' concept and intermetallic phases. Kaufman (1967) and Kaufman and Bernstein (1970) constructed many different phase diagrams using ideal or regular solution theory and assessed values for the energy differences between the f.c.c., b.c.c. and c.p.h. phases for many elements. The work clearly demonstrated that the correct forms of phase diagrams could be matched with simple concepts and models. Although these diagrams cannot now be considered accurate enough for detailed application, there is little doubt that correct trends were predicted, and this more than anything confirmed the validity of a number of the fundamental concepts of the CALPHAD route.

Probably the most fundamental change in modelling, particularly in the solid state, has occurred through the development and application of the sub-lattice model (see Chapter 5). In early years the mathematical formalisms for describing substitutional solid solutions had been well established and it was these types of models which were first employed for phases such as the B2, NiAl phase in Ni–Al (Kaufman and Nesor 1978b) (Fig. 10.5) and the σ phase in Cr–Fe (Chart *et al.* 1980) (Fig. 10.6). Otherwise intermetallic compounds were usually treated as line compounds (Figs 10.5 and 10.7). The disadvantages of both models are substantial. Firstly, in multi-component space it is difficult to model properties of compounds which have preferred stoichiometries and sub-lattice occupation, using a model which essentially describes random mixing on a single sub-lattice. Secondly, in

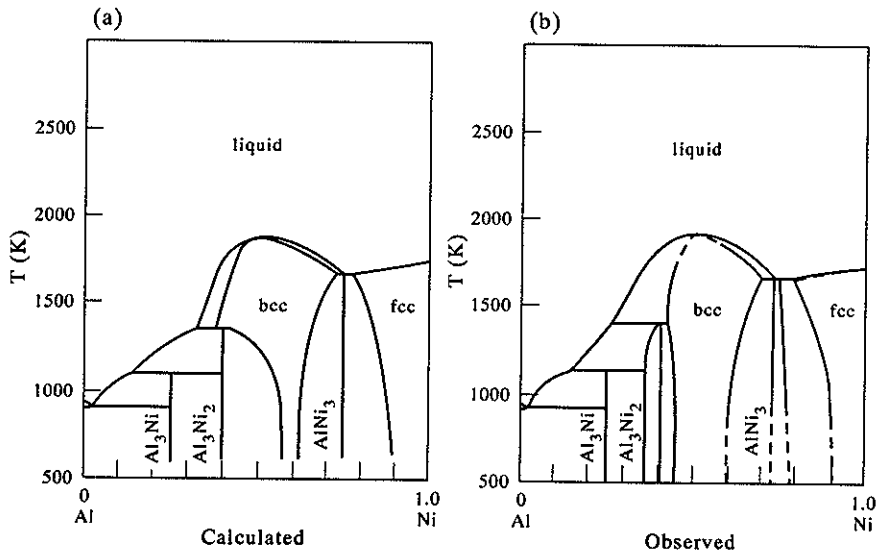

Figure 10.5 (a) Calculated and (b) observed Ni–Al phase diagram (from Kaufman and Nesor 1978b).

References are listed on pp. 402–408.

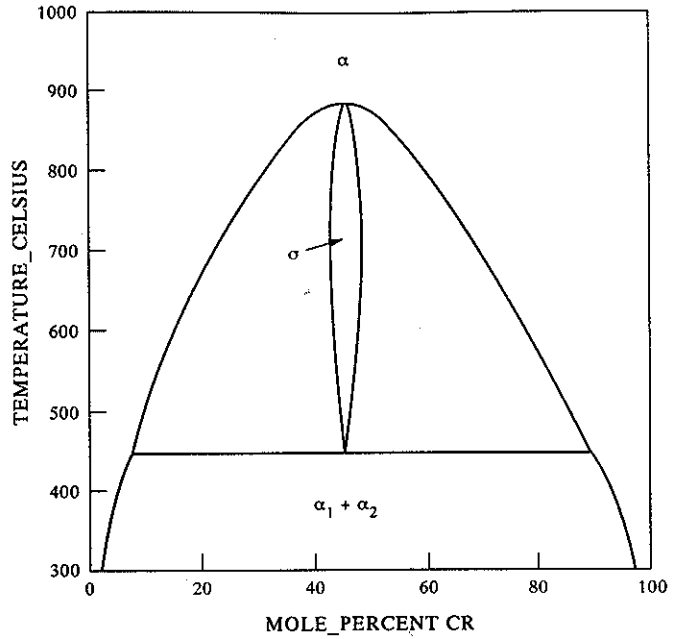

Figure 10.6 Calculated low-temperature region of the Cr–Fe system (Chart *et al.* 1980).

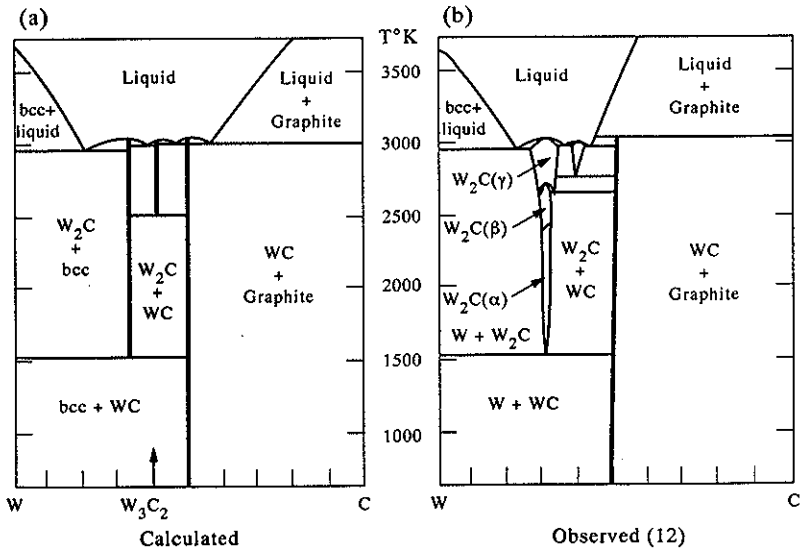

Figure 10.7 (a) Calculated and (b) observed W–C phase diagram (from Kaufman and Nesor 1978a).

systems where solubility ranges are very important, for example the γ' phase in Ni-based superalloys, the stoichiometric compound approach can never achieve high levels of accuracy.

The sub-lattice model is now the predominant model used in most CALPHAD calculations, whether it be to model an interstitial solid solution, an intermetallic compound such as γ-TiAl or an ionic solution. Numerous early papers, often centred around Fe–X–C systems, showed how the Hillert–Staffansson sub-lattice formalism (Hillert and Staffansson 1970) could be applied (see for example Lundberg *et al.* (1977) on Fe–Cr–C (Fig. 10.8) and Chatfield and Hillert (1977) on Fe–Mo–C (Fig. 10.9)). Later work on systems such as Cr–Fe (Andersson and Sundman 1987) (Fig. 10.10) showed how a more generalised sub-lattice treatment developed by Sundman and Ågren (1981) could be applied to multi-sub-lattice phases such as σ.

Alongside calculations for alloy systems, complex chemical equilibria were also

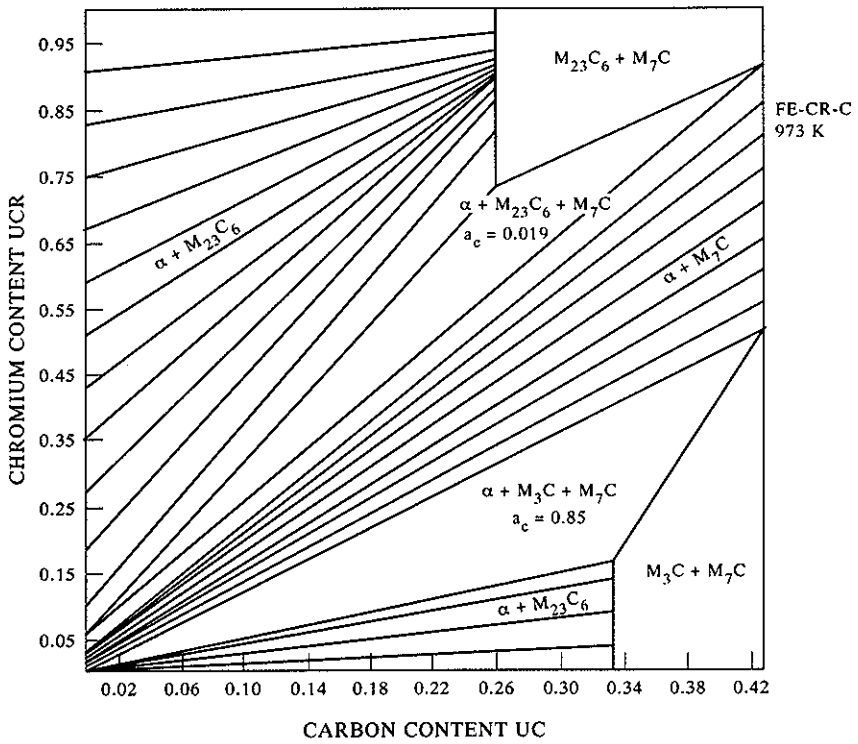

Figure 10.8 Calculated isothermal section for Fe–Cr–C at 973 K (Lundberg *et al.* 1977). Axes are in U-fractions where UCR = $x_{Cr}/(1-x_C)$ and UC = $x_C/(1-x_C)$.

References are listed on pp. 402–408.

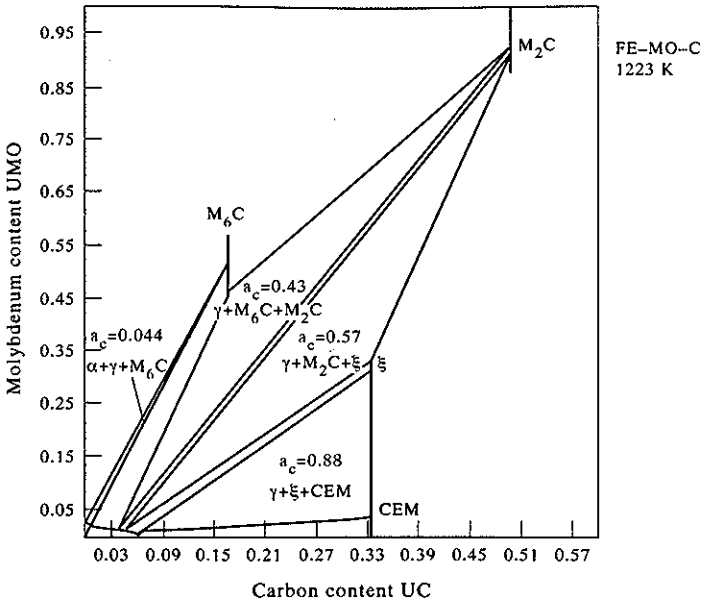

Figure 10.9 Calculated isothermal section for Fe–Mo–C at 1223 K (Chatfield and Hillert 1977). Axes are in U-fractions where UMO = $x_{Mo}/(1-x_C)$ and UC = $x_C/(1-x_C)$.

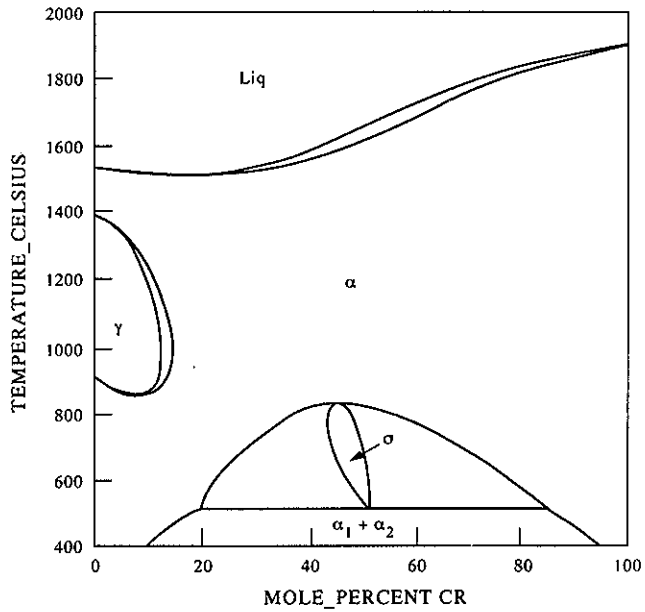

Figure 10.10 Calculated Cr–Fe phase diagram (Andersson and Sundman 1987).

being dealt with on a routine basis. These calculations centred around so-called 'substance' databases, which include data for condensed, stoichiometric substances and an ideal gas phase containing many different species. In essence, the computational aspects of such calculations are less severe than for alloy or ionic systems which are dominated by more complex models. However, they have a complexity of their own as the input of only a few elements gives rise to substantial numbers of substances and gaseous species. For example, in a gas-phase reaction involving C–H–N–O there could be some 60 various gaseous species. Furthermore, in fields such as environmental studies, it is important to consider low levels of activity, so it is not always possible to simplify the potential reactions by 'suspending' species if they exist below a certain critical limit.

The simplicity of modelling in 'substance'-type calculations meant that complex systems could be studied at an early stage of CALPHAD development. The SolGasMix programme of Eriksson (1975) was one of the first to provide such a capability, and within a decade very complex systems were being routinely handled; two good examples are given in the CALPHAD volume dedicated to Eriksson in 1983. Lindemer (1983) was able to look at gas-phase reactions in a fission reaction involving U–Cs–I–Ba–Zr–Mo considering 18 gaseous species and 20 condensed substances. Another interesting example of a calculation based mainly on a substance database is given in the work of Lorenz *et al.* (1983) who were interested in the stability of SiC-based ceramics containing ZrO_2 and other oxides. This involved the quaternary system $SiC–ZrO_2–Al_2O_3–SiO_2$ reacting in inert argon gas, and gave rise to 36 gaseous species and 22 stoichiometric, solid substances. Calculations of the reaction for various composite mixtures of SiC and oxides were then made as functions of temperature and pressure. Calculations involving so many phases were not being routinely handled at this time for systems such as steels, where non-ideal mixing in most of the solid phases is the norm.

There now exists a thriving community of researchers who regularly publish thermodynamic assessments for binary and ternary systems. Many are extremely accurate and, due to a formalisation of unary data proposed by SGTE (Dinsdale 1991), these can be combined with existing or future work in the establishment of multi-component solution databases, where the promise of CALPHAD methods is greatest. In many ways an accurate thermodynamic assessment of a binary or ternary system only proves again the validity of the fundamental concepts laid down in earlier years. The models have improved and, therefore, levels of accuracy level have improved, but most commonly used materials are multi-component in nature and the degree to which binary and ternary assessments can be applied *per se* is fundamentally limited. The key issue is how to extend the CALPHAD route to 'real' rather than 'ideal' materials, and the next section will concentrate on this issue.

References are listed on pp. 402–408.

10.3. GENERAL BACKGROUND TO MULTI-COMPONENT CALCULATIONS

10.3.1 Introduction

From their earliest days CALPHAD methods have always promised to be extendable to complex materials. Certainly, the necessary mathematical formulations to handle multi-component systems have existed for some time and have been programmed into the various software packages for calculation of phase equilibria. However, it is interesting to note that, until quite recently (with the exception of steels), there has been little actual application to complex systems which exist in technological or industrial practice, other than through calculations using simple stoichiometric substances, ideal gas reactions and dilute solution models. The latter have been used for some time, as it is not intensive in computational terms, and some industrially important materials, although containing many elements, are actually low in total alloy or impurity content, e.g., HSLA steels. Examples in this area can be found in Kirkaldy *et al.* (1978), Bhadeshia and Edmond (1980), Hack and Spencer (1985) and Kroupa and Kirkaldy (1993). The limitations of dilute solution models have been discussed earlier in Chapter 5 and, although useful for certain limited applications, they are not applicable in a generalised way and could not begin to handle, with any accuracy, complex alloy types such as stainless steels or Ni-based superalloys. Substance calculations, while containing large numbers of species and condensed phases, are, in many ways, even more limited in their application to alloys as they do not consider interactions in phases involving substantial mixing of the components.

The main areas of application for more generalised models have, until recently, been restricted to binary and ternary systems or limited to 'ideal industrial materials' where only major elements were included. The key to general application of CALPHAD methods in multi-component systems is the development of sound, validated thermodynamic databases which can be accessed by the computing software and, until recently, there has been a dearth of such databases.

The notable exception to this trend was steels and, in particular, stainless and high-speed steels where alloy contents can rise to well above 20wt%. For such alloys a concentrated solution database (Fe-base) has existed since 1978, based on work done at the Royal Institute of Technology (KTH), Stockholm, Sweden. However, although it is far more generalised than dilute solution databases, its range of applicability is limited in temperature to between 700° and 1200°C. Work since 1978, mainly by the Royal Institute of Technology, has seen the development of a new steel database, TCFe, for use in Thermo-Calc. This work now forms the basis for steel calculations in the SGTE solution database. More recently, TCFe has been extended and improved by Saunders and Sundman (1996). These newer databases have a number of distinct advantages over the old Fe-base, not least in that liquid-phase equilibria is now taken into account.

The lack of similar databases for other material types presented severe problems

for CALPHAD calculations with any of the other commonly used materials and led to a concentration of application to steels. However, in the past four years further multi-component databases have been developed for use with Al-, Ni-, Ti- and TiAl-based alloys (Saunders 1996a–c, 1997a,b). These databases have been created mainly for use with industrial, complex alloys and the accuracy of computed results has been validated to an extent not previously attempted. Simple, statistical analysis of average deviation of calculated result from experimental measurement in 'real', highly alloyed, multi-component alloys has demonstrated that CALPHAD methods can provide predictions for phase equilibria whose accuracy lies close to that of experimental measurements.

The importance of validation of computed results cannot be stressed too highly. We are now in a position where computational speed has allowed the development of modelling in many related areas. These models often rely on input data which can be time-consuming to measure but can be readily predicted via CALPHAD and related methods. Therefore, CALPHAD results may be used as input for other models, for example, in the manufacture of a steel starting from the initial stages in a blast furnace, through the refinement stages to a casting shop, followed by heat treatment and thermomechanical processing to the final product form. All of these stages can be modelled and all use input data which can be provided either directly or indirectly from CALPHAD calculations. Such a future total modelling capability will never materialise properly until confidence can be placed in the predictions of each of the building blocks. In the case of CALPHAD methods, the key to this is the availability of high-quality databases and the rest of this section will concentrate on databases and discuss some of the strategies in their construction.

10.3.2 Databases

10.3.2.1 'Substance' databases. Basically substance databases have little complexity as they are assemblages of assessed data for stoichiometric condensed phases and gaseous species. They have none of the difficulties associated with non-ideal mixing of substances, which is the case for a 'solution' database. However, an internal self-consistency must still be maintained. For example, thermodynamic data for $C_{(s)}$, $O_{2<g>}$ and $CO_{2<g>}$ are held as individual entries, which provide their requisite properties as a function of temperature and pressure. However, when put together in a calculation, they must combine to give the correct Gibbs energy change for the reaction $C_{(s)}+O_{2<g>}=CO_{2<g>}$. This is a simple example, but substance databases can contain more than 10,000 different substances and, therefore, it is a major task to ensure internal self-consistency so that all experimentally known Gibbs energies of reaction are well represented. Examples of substance databases of this type can be found in the review of Bale and Eriksson (1990).

References are listed on pp. 402–408.

10.3.2.2 'Solution' databases. Solution databases, unlike substance databases, consider thermodynamic descriptions for phases which have potentially wide ranges of existence both in terms of temperature and composition. For example, the liquid-phase can usually extend across the whole of the compositional space encompassed by complete mixing of all of the elements. Unlike an ideal solution, the shape of the Gibbs energy space which arises from non-ideal interactions can become extremely complex, especially if non-regular terms are used. Although it may seem an obvious statement, it is nevertheless important to remember that thermodynamic calculations for complex systems are multi-dimensional in nature. This means that it becomes impossible to visualise the types of Gibbs energy curves illustrated in earlier chapters which lead to the easy conceptualisation of miscibility gaps, invariant reactions, etc. In multi-component space such things are often difficult to understand, l*et al*one conceptualise. Miscibility gaps can appear in ternary and higher-order systems even though no miscibility gap exists in the lower-order systems. The Gibbs phase rule becomes vitally important in understanding reaction sequences, but often one has to accept the computer predictions which can be surprising at times. This emphasises the need to validate the database for multi-component systems and leads inexorably to the concept of two types of database.

10.3.3 The database as a collection of lower order assessments

Essentially this is the basic concept of any database, but an unthinking application of this concept is dangerous. It can be easily demonstrated that in multi-component calculations the properties of some substances, or lower-order interactions in solution phases, are ineffective in modifying phase equilibria, while in other cases some are extremely critical. This may be because the total energy of the system is very exothermic and a particular Gibbs energy term is close to ideal. In this case a change of a few hundred percent in a binary value actually alters things very little. Other reasons may exist for the precise value of an interaction being non-critical. For example, the equilibrium solubility of elements in a particular phase may be small and the $\sum_i \sum_j x_i x_j$ solubility product subsequently produces small changes in total energy, even if interaction coefficients are heavily modified. This leads to a number of important questions and concepts. The first and most important question is how many of the constituent substances or lower-order interactions must be accurately represented before a successful calculation can be guaranteed.

Let us take the example of a simple commercial alloy such as Ti–6Al–4V. This is the most popular structural Ti alloy used worldwide. Essentially one would need to consider Ti–Al, Ti–V and Al–V binary interactions and Ti–Al–V ternary interactions. Unfortunately, although called Ti–6Al–4V, this alloy also contains small amounts of O, C, N and Fe and it therefore exists in the multi-component space within the Ti–Al–V–O–C–N–Fe system. There are then 21 potential binary

interactions and 35 possible ternary interactions to consider. The number of thermodynamic assessments necessary to obtain all of these parameters is obviously massive, and the inclusion of an additional element to the alloy means a further 7 binary and 21 ternary assessments would potentially need to be made. This would make a total of 28 binary and 56 ternary assessments. The effort to do all of this is so large that it is much easier (and cheaper) to consider an almost exclusively experimental route to determining phase equilibria in the commercial Ti–6Al–4V alloy. This can be enhanced with regression analysis techniques to specify the effect of various elements on critical features such as the temperature when the alloy becomes fully β.

Fortunately, it is not necessary to perform all of these thermodynamic assessments. In essence one should ensure that all of the binary systems are completed, but the levels of C and N are so low that it is possible to effectively ignore interaction parameters between these two elements, even if they were possible to determine. The percentage of ternary assessments which is necessary to provide an accurate calculation is, in reality, small, mainly because the ternary $\sum_i \sum_j \sum_k x_i x_j x_k$ solubility product can be small for the minor elements. For example, the effect of including ternary parameters for Fe–C–N, which are basically impurity elements, is negligible and little effect is found from the Fe–V–N system even though it contains one of the major elements.

It can therefore be seen that if we wish to consider making calculations for the Ti–6Al–4V alloy, the actual amount of work is much reduced from the theoretical number of permutations. However, this is a particularly simple Ti-alloy and another type such as IMI 834 typically contains Ti, Al, Sn, Zr, Nb, Si, C, O, N and Fe, where seven elements have a significant effect on phase equilibria. The general problem, therefore, remains as to how to judge the number of the potential interactions which must be included, so that a successful multi-component calculation can be made. This cannot be answered in a simple fashion and the position is considerably exacerbated if one wishes to make a generalised database applicable for many material types. If reliable and accurate multi-component calculations are to be made, new paradigms are required and it is no longer possible to consider using databases which are basically constructed as collections of assessed binary and ternary systems which might be available at the time. *The database itself must be assessed.*

10.3.4 Assessed databases

By definition 'assessed databases' are focused, usually on material types. The recent Al-, Ni- and Ti-databases (Saunders 1996a–c) and, to a large degree, the Fe-databases produced by KTH in Stockholm are good examples. They contain up to 15 elements and have been designed for use within the *composition space* associated with the different material types. All, or most, of the *critical* binary and ternary systems have been assessed and calculated results have been *validated* as being successful. The words italicised in the previous sentence hold the key paradigms which need to be employed when designing an assessed database.

Composition space. It is firstly of critical importance that a well-understood and properly circumscribed composition space is defined. This is best done by considering databases for use with particular material types, for example steels, conventional Ti alloys, etc. This firstly limits the number of elements which need to be considered and also helps to define concentration limits for these elements.

Critical systems. It is impossible just by looking at a list of elements to decide which are the critical binary and ternary systems that must be critically assessed. However, some clear pointers can be gained by looking at the composition space in which the database is to be used. For example, B levels in Ni-based superalloys as a rule do not exceed 0.1wt% and, therefore, assessment of B-rich ternary and higher-order alloys is unnecessary. There are, however, critical B-containing ternary systems which must be assessed to understand the thermodynamics of the M_3B_2 phase which can appear. Likewise, the thermodynamics of the MC carbide must be well defined and this includes a large number of carbon-containing ternary systems. On the other hand, although Ti, Ta and Nb may appear in the alloy in much larger amounts than B and C, a ternary assessment of Ti–Ta–Nb is not critical as the magnitude of the thermodynamic interactions are small which, combined with the $\sum_i \sum_j \sum_k x_i x_j x_k$ solubility product term, makes for small Gibbs energy changes. The understanding of the critical systems in an assessed database is in the hands of the developer of the database and can often only be understood after a series of multi-component calculations are made.

Validation of the database. This is the final part in producing an assessed database and must be undertaken systematically. There are certain critical features such as melting points which are well documented for complex industrial alloys. In steels, volume fractions of austenite and ferrite in duplex stainless steels are also well documented, as are γ' solvus temperatures (γ'_s) in Ni-based superalloys. These must be well matched and preferably some form of statistics for the accuracy of calculated results should be given.

Only after at least these three steps are taken can a database then be considered as an assessed database and used with confidence in an application involving a complex multi-component alloy.

10.4. STEP-BY-STEP EXAMPLES OF MULTI-COMPONENT CALCULATIONS

This section will take three commercial alloys and analyse how the final calculated result took form, starting with some of the important constituent binary and ternary diagrams, and seeing how the various features of the final alloy are controlled by these underlying systems.

References are listed on pp. 402–408.

10.4.1 A high-strength versatile Ti-alloy (Ti–6Al–4V)

Ti–6Al–4V is probably the most widely used Ti alloy in the world. It is an alloy with a duplex structure containing solid solutions based on the α, c.p.h._A3 and β, b.c.c._A2 allotropes of Ti. In its final heat-treated form it consists predominantly of α and its high strength is partly derived from its final microstructure which is manipulated by a series of thermomechanical treatments that include hot isothermal forging just below its β transus temperature (T^{β}). The interest is, in the first place, to predict T^{β} and how the amounts of α and β vary with temperature.

There are empirical relationships which relate alloy content to T^{β}, but these are not usually applicable to all types of Ti alloy and can suffer from a lack of accuracy. Significantly, there are no such relationships which can be generally used for predicting the amount of α and β in commercial alloys as a function of temperature and composition and little work has been undertaken to quantitatively understand the partitioning of elements between the α and β phases.

The alloy combines the features of two different binary systems, Ti–Al and Ti–V (Figs 10.11 and 10.12). Al is an 'α-stabiliser' while V is a strong 'β-stabiliser'. It is the combination of these two types of diagram which produces a wide two-phase $\alpha + \beta$ region, and Fig. 10.13 shows the behaviour of the basic ternary alloy as a function of temperature. Although more heavily alloyed in Al, the alloy never

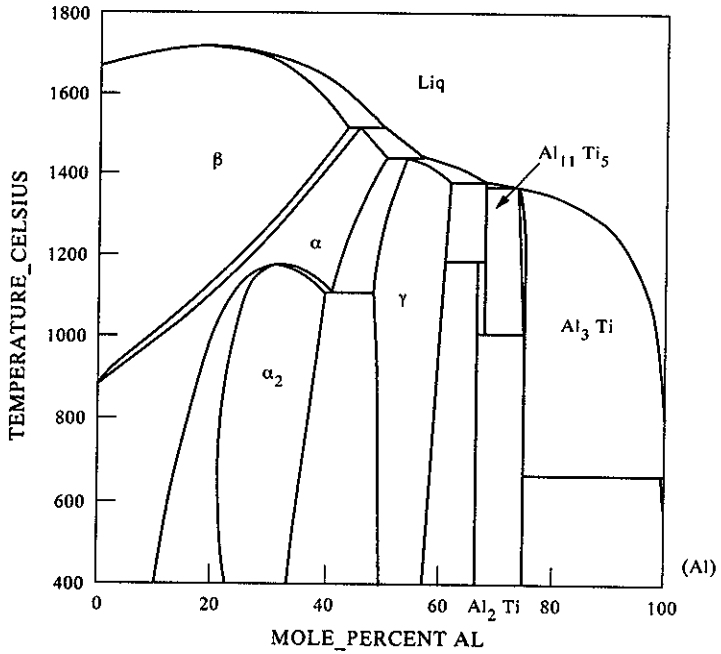

Figure 10.11 Calculated Ti–Al phase diagram.

References are listed on pp. 402–408.

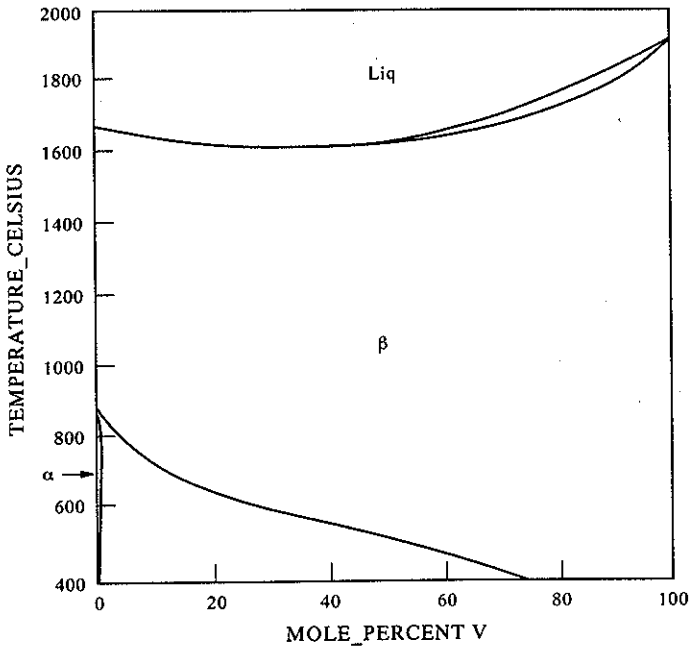

Figure 10.12 Calculated Ti–V phase diagram.

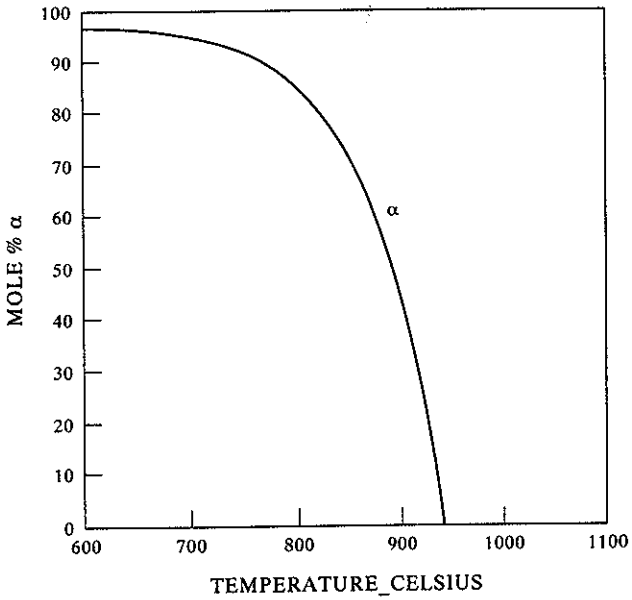

Figure 10.13 Calculated mole % α vs temperature plot for a Ti–6Al–4V ternary alloy.

becomes fully α, as just enough V is added to retain some β. The basic behaviour of the alloy is thus defined by the Ti–Al–V ternary but Ti alloys always contain significant levels of O and N, and in the case of Ti–6Al–4V usually some Fe. At high levels (>5000 ppm) O generally acts as an embrittling agent, but at lower levels (2000 ppm) it can be used to enhance strength (Jaffee 1958) and is therefore a deliberate addition to 'conventional' alloys such as Ti–6Al–4V. Apart from the physical effects of O, this also produces significant phase-boundary shifts even at low levels of uptake, and it is therefore necessary to include the effects of at least this element in the calculations.

Figure 10.14 shows the calculated Ti–O diagram from Lee and Saunders (1997). In the composition range of interest it is of a simple type but O has a powerful effect on T^{β}. This effect is carried over to the critical ternary system Ti–Al–O and Figs 10.15 and 10.16 show how the Ti–Al system changes as O is added (Lee and Saunders 1997). No such information is available for Ti–V–O but it is interesting to note the predicted effect of O on Ti–V. Figure 10.17 shows a section through

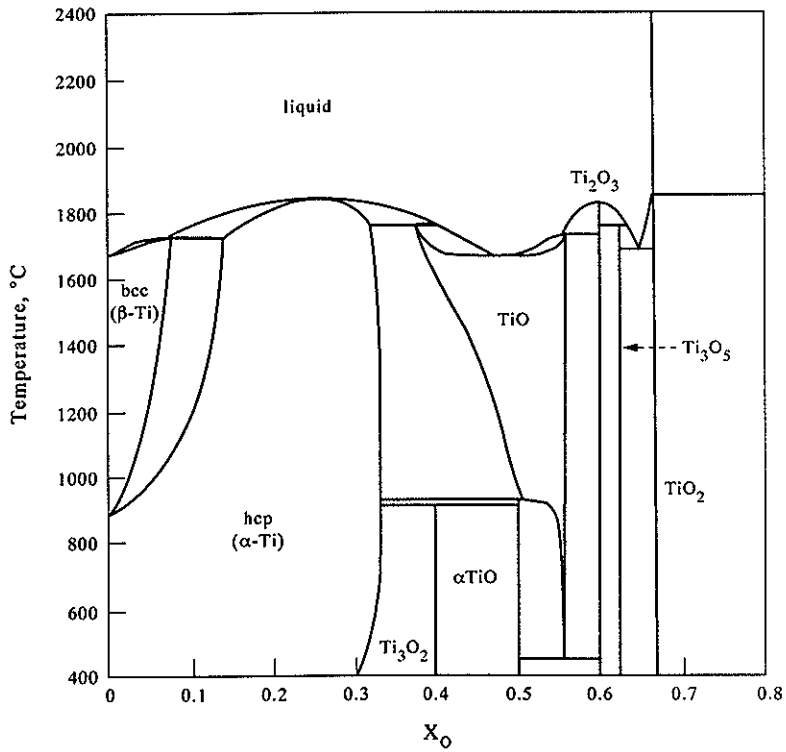

Figure 10.14 Calculated Ti–O phase diagram (from Lee and Saunders 1997).

References are listed on pp. 402–408.

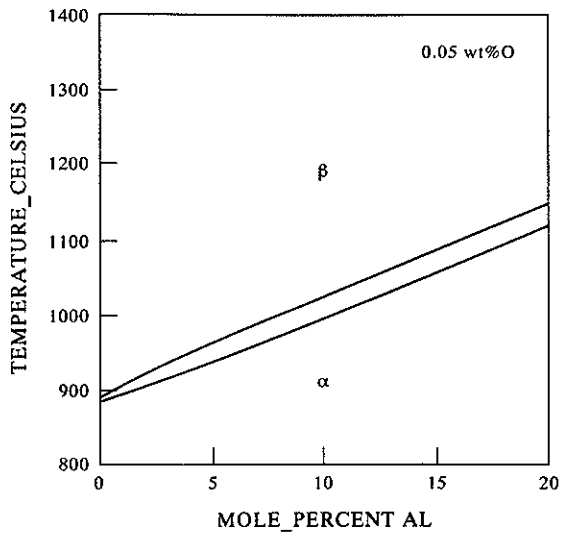

Figure 10.15 Calculated vertical section through Ti–Al–O at 0.05wt%O.

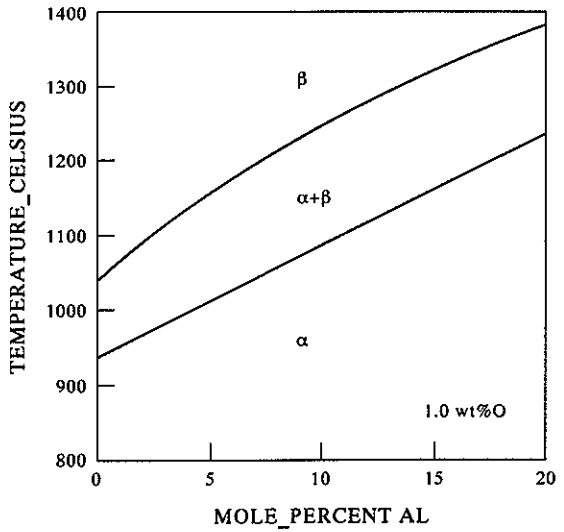

Figure 10.16 Calculated vertical section through Ti–Al–O at 1.0wt%O.

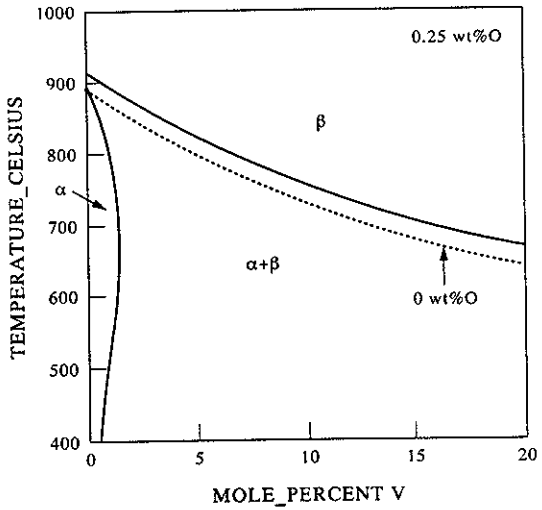

Figure 10.17 Calculated vertical section through Ti–V–O at 0.25wt%O.

Ti–V–O at a constant 2500 ppm of O and the effect of O on T^{β} is significant, while the effect on the position of the α-phase boundary is minimal.

Taking the necessary binary assessments for the inclusion of C, N and Fe and the assessments for Ti–Al–O and Ti–V–O, the effect of O on the T^{β} of Ti–6Al–4V with typical C, N and Fe impurity levels, was calculated and compared with experiment. The agreement between the calculations and experimental results of Kahveci and Welsch (1986) is good (Fig. 10.18). Figure 10.19 further shows some calculated phase % vs temperature plots for three Ti–6Al–4V commercial alloys and compares these with experiment. The advantage of the CALPHAD route becomes increasingly apparent because, as well predicting T^{β}, the calculations have also given good results for the amounts of α and β.

Furthermore, it is now possible to look at the partitioning of the various elements to the α and β phases and Fig. 10.20 shows comparisons with experiment for the various metallic elements. One of the V results for the β phase has an arrow indicating that the true experimental result was considered to be higher than that shown in Fig. 10.20 (Lasalmonie and Loubradou 1979). This is because the β grains were so small that some overlap with the α matrix occurred during measurement by EPMA, resulting in a V reading that is almost certainly too low.

As previously stated, the levels of the light elements such as O are important in determining physical properties of Ti and it is also possible to look at the partitioning of O between the α and β phases (Fig. 10.21). It can be seen that the level of O in α just below T^{β} is extremely high. This has significant consequences for thermomechanical processing for Ti–6Al–4V at these temperatures as yield

References are listed on pp. 402–408.

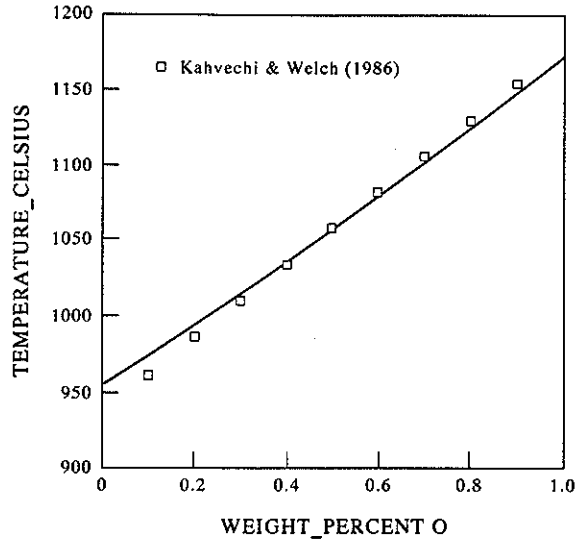

Figure 10.18 Comparison between calculated and observed β-transus for Ti–6Al–4V alloys as a function of O concentration.

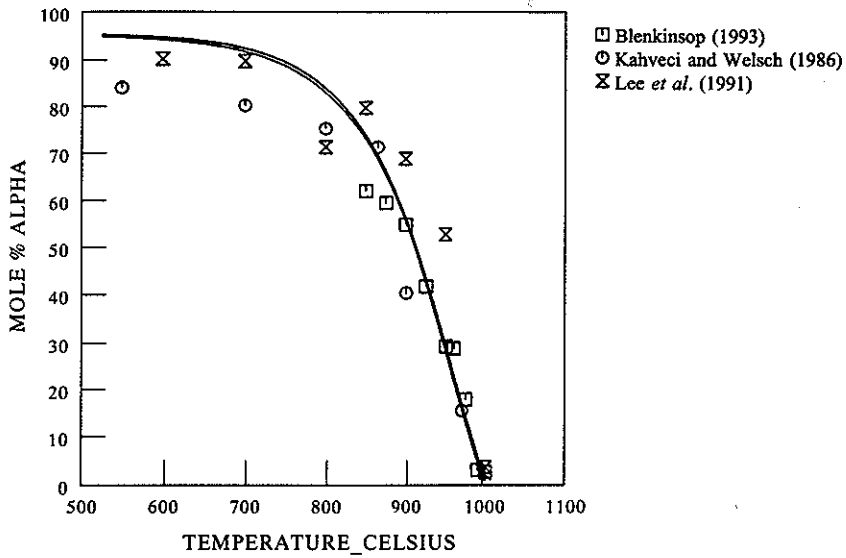

Figure 10.19 Calculated mole % phase vs temperature plots for three Ti–6Al–4V alloys with experimental data superimposed.

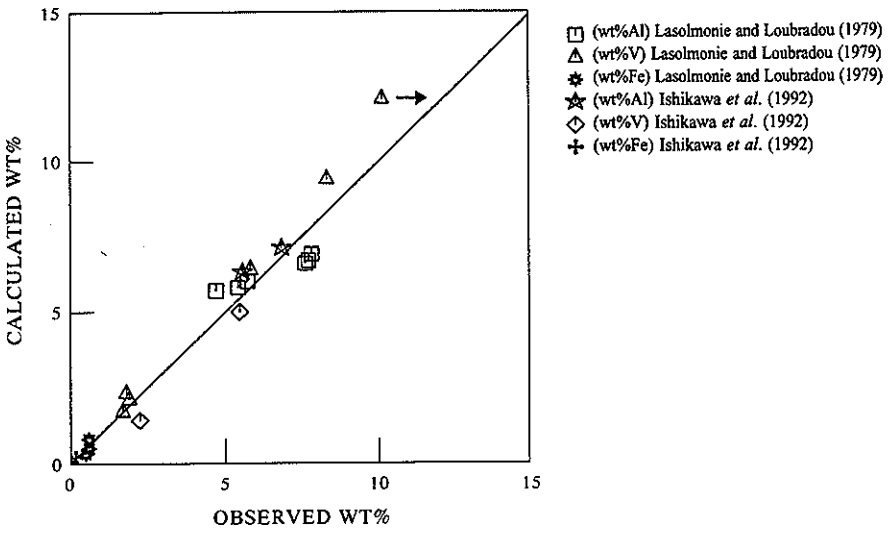

Figure 10.20 Comparison between calculated and experimental values for the concentration of Al, V and Fe in the α and β phase in Ti–6Al–4V alloys.

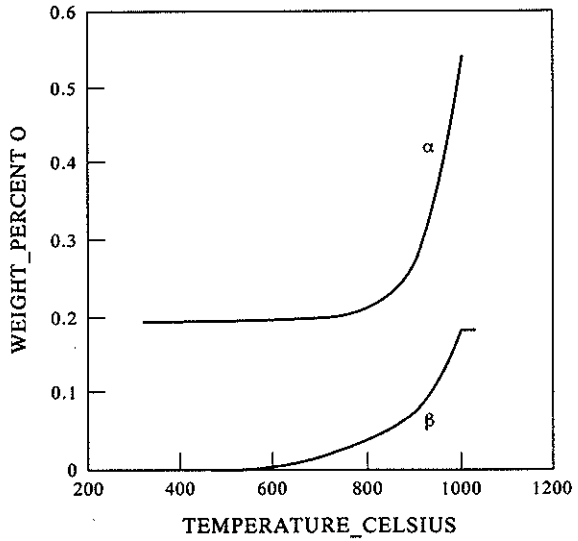

Figure 10.21 Calculated concentration of O in the α and β phase for a Ti–6Al–4V alloy.

References are listed on pp. 402–408.

strengths in α will be higher and ductility levels lower than would be expected by just taking total levels of impurity as a guide.

10.4.2 A high-tonnage Al casting alloy (AA3004)

Aluminium alloys form one of the most widely used groups of materials in existence. They make products which are often cheap and can be applied to many different areas. Extensive work has been done on the experimental determination of binary and ternary phase diagrams, mainly during the mid-part of this century, and researchers such as Phillips (1961) and Mondolfo (1976) have produced detailed reviews of the literature which provide industry standard publications. However, although some important Al-alloys are based on ternary systems, such as the LM25/356 casting alloy based on Al–Mg–Si, in practice they inevitably include small amounts of Cu, Mn, Fe, Ti etc., all of which can significantly modify the castability and properties of the final product. The situation is further exacerbated by the use of scrap material. It is therefore useful to be able to predict phase equilibria in multi-component alloys.

The modelling issues for Al alloys turn out to be reasonably straightforward. Unlike superalloys or steels there are few intermetallic phases with wide regions of stoichiometry. A large number of the compounds tend to be stoichiometric in nature, for example, Mg_2Si and Al_2CuMg. Where there is substantial solubility, such as in the Al_6Mn and α-AlFeMnSi phases, the transition metals basically mix on one sub-lattice while Si mixes on the Al sub-lattice. The phases can be then treated as conventional line compounds and complexities of modelling associated with phases such as σ and γ', where many elements may mix on more than one sub-lattice, do not arise. There is also limited solubility in the Al solid solution for most elements which are usually added to Al alloys which means that, for this phase, the effect of most ternary interactions is completely negligible. Nevertheless, Al alloys more than make up for this simplicity in modelling by exhibiting reaction schemes which can be far more complex than usually found in systems involving more complex models. Because of their inherent simplicity in modelling terms, Al systems offer a good example of how a database can be constructed and the AA3004 alloy, which is based on the Al–Fe–Mn–Si system, will now be discussed in more detail.

The Al–Si diagram and Al-rich regions of the Al–Mn and Al–Fe diagrams are shown in Figs 10.22–10.24. The Al–Mn and Al–Fe systems are modifications based on the work of Jansson (1992) and Saunders and Rivlin (1987). Unless stated, all other diagrams are from Saunders (1996b). The Al–Mn and Al–Fe diagrams are complex but in terms of Al alloys only the Al_6Mn, Al_4Mn and Al_3Fe phases are of importance. This leads to a large degree of simplification in considering the ternary modelling.

Figure 10.25 shows the liquidus projection for the Al–Fe–Mn system which is characterised by a substantial extension of the Al_6Mn phase into the ternary and

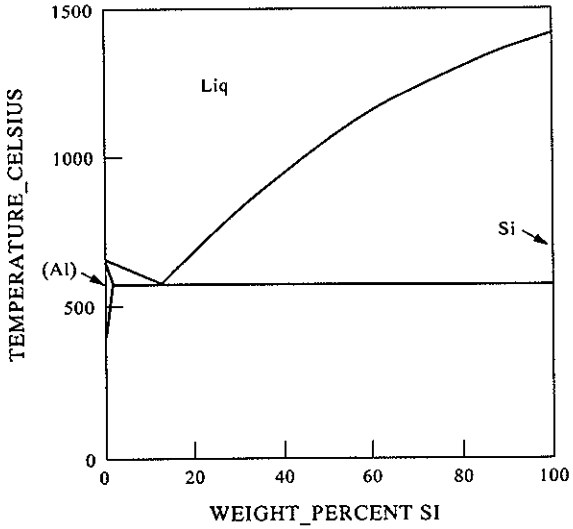

Figure 10.22 Calculated Al–Si phase diagram.

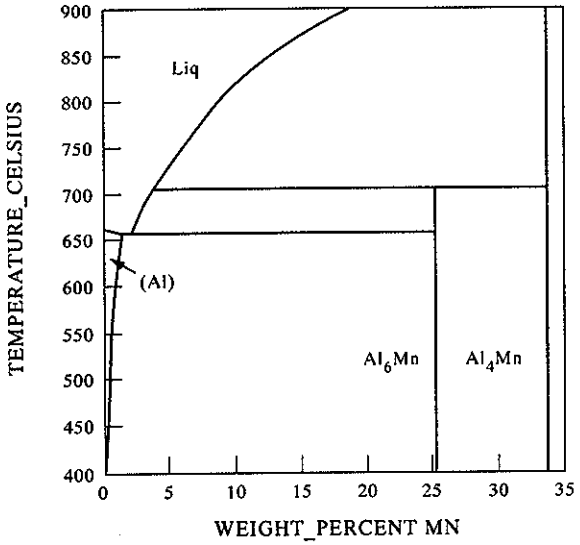

Figure 10.23 Calculated Al-rich region of the Al–Mn phase diagram.

References are listed on pp. 402–408.

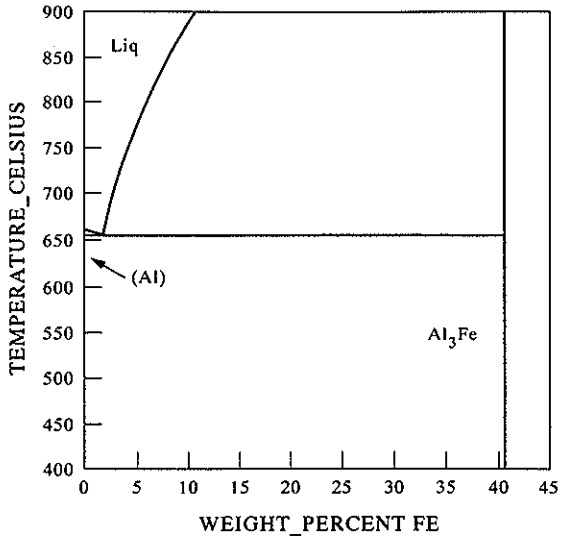

Figure 10.24 Calculated Al-rich region of the Al–Fe phase diagram.

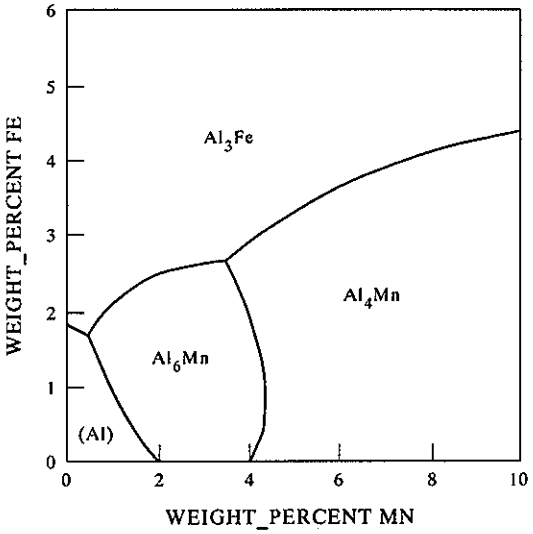

Figure 10.25 Calculated liquidus projection for Al–Fe–Mn.

some slight uptake of Mn in Al_3Fe. These extensions basically comprise Mn and Fe substitution in an otherwise stoichiometric compound. The diagram has been reviewed by Phillips (1961) and Mondolfo (1976) where there is good agreement on features such as the eutectic temperature and compositions of phases. The main problem with the assessment of Al systems is in interpretation of experimental information concerning the liquidus of the compounds, where results can be scattered. This is a general problem and relates partly to the steepness of the liquidus slope and the low solubility of some transition elements in liquid Al. Such liquidus lines are difficult to determine accurately by methods such as DTA, as there is often very little heat associated with the transformation, and significant undercooling can also occur. The most reliable measurement techniques tend to be isothermal in their nature, for example, sampling of the liquid.

The addition of Si to Al–Mn and Al–Fe leads to the formation of a number of ternary compounds (Figs 10.26 and 10.27). There is significant mixing between Al and Si in the cubic α-AlMnSi phase but the other phases are treated accurately as compounds with fixed stoichiometry. The agreement between the calculated diagrams and those of Phillips (1961) and Mondolfo (1976) is again good, with compositions of invariant reactions typically being to within 1 wt% of each element and 5°C in temperature.

The joining of the ternary systems into Al–Fe–Mn–Si basically involves considering the α-AlMnSi compound which extends almost completely to Al–Fe–Si. In fact, in early work on Al–Fe–Si alloys, which contained minor levels of Mn, the

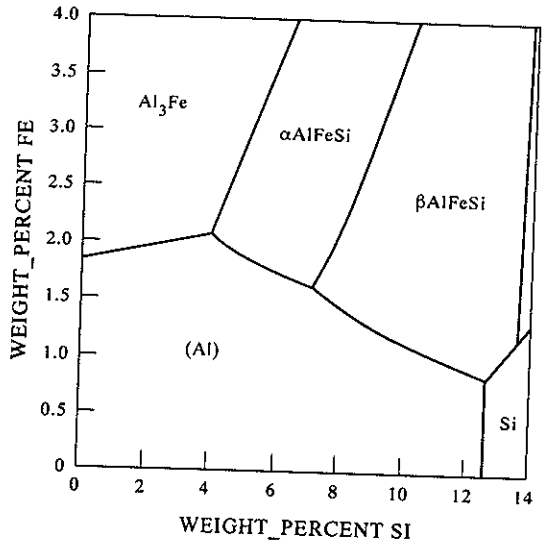

Figure 10.26 Calculated liquidus projection for Al–Fe–Si.

References are listed on pp. 402–408.

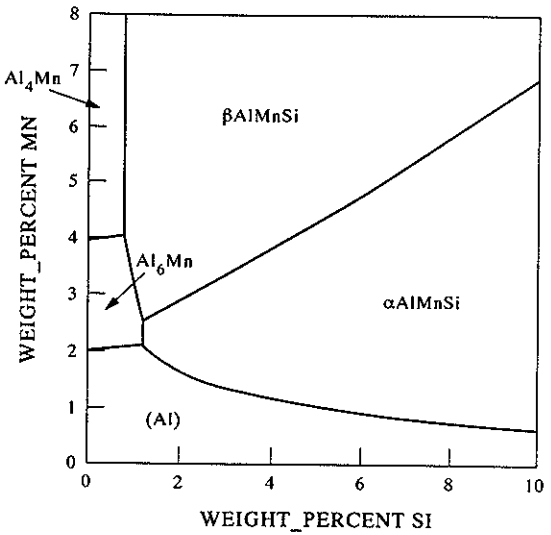

Figure 10.27 Calculated liquidus projection for Al–Mn–Si.

α-AlFeSi phase was considered to be isomorphous with α-AlMnSi. Later work showed this not to be the case and its stable structure is hexagonal (Munson 1967, Mondolfo 1976, Rivlin and Raynor 1988). The addition of Fe to the α-AlMnSi phase is simply achieved by making the Gibbs energy of the cubic AlFeSi compound only just metastable. Other elements such as Cr and V also partition to the cubic α phase and this can also be taken into account.

Combining this quaternary with Mg, and in particular Al–Mg–Si, it is now possible to consider a reasonably pure AA3004 alloy which is used extensively for thin-walled containers such as drink cans. Figures 10.28(a,b) show phase % vs temperature plots for an alloy Al–1Mn–1.2Mg–0.5Fe–0.2Si (in wt%). On solidification the primary phase is Al, with Al_6Mn appearing soon afterwards. There is a subsequent peritectic reaction involving α-AlFeMnSi (which will now just be called α) which partly consumes the Al_6Mn phase. The amount of α increases as the alloy is cooled below its solidus and it becomes the dominant solid-state intermetallic just below 600°C. However, it disappears around 400°C, as Si is taken up by the formation of Mg_2Si which acts as a precipitation hardening phase. The interplay between the α and Al_6Mn is critical, as the surface finish during fabrication of cans is much improved if α particles, rather than Al_6Mn, predominate in 3XXX alloys of this type (Anyalebechi 1992, Marshall 1996). It is therefore now possible for CALPHAD methods to be used as a tool in helping to model and control this reaction.

Cama *et al.* (1997) studied an alloy with the same composition as used in the last

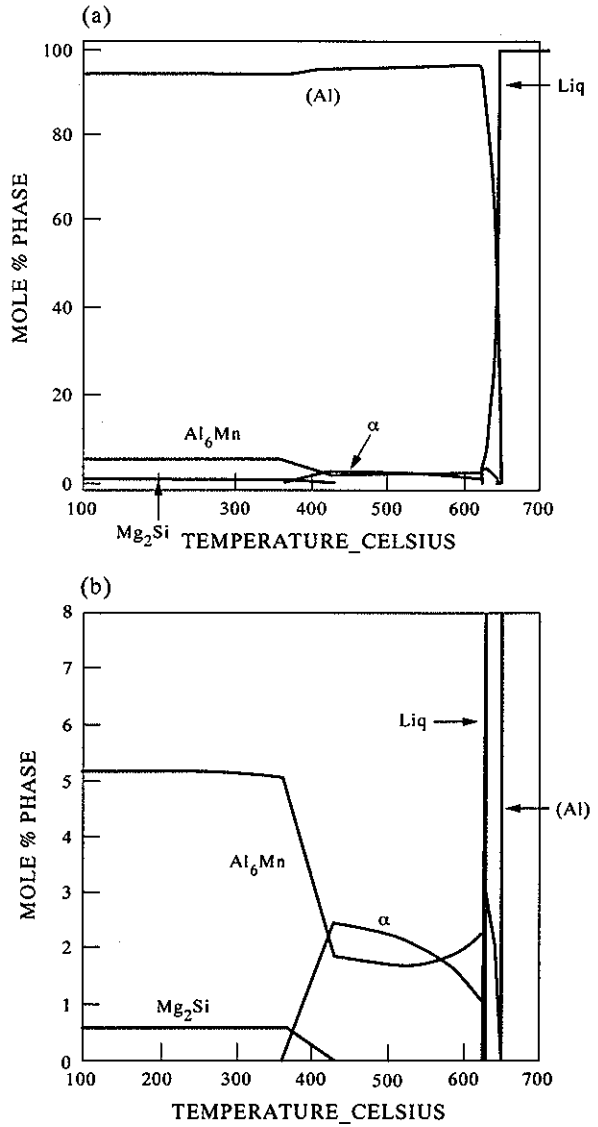

Figure 10.28 (a) Calculated mole % phase vs temperature plot for a AA3004 alloy. (b) Expanded region of Fig. 10.26(a).

calculation, but with 0.2wt%Cu added, and performed long-term anneals between 550° and 630°C. They measured the relative levels of Al_6Mn and α and reported results as a percentage of α observed. Calculations were therefore made for their

References are listed on pp. 402–408.

alloy so that computed results could be compared with experiment. Experimental results varied between 61 and 39% while the calculations predict values of 53–33%. The calculations suggest some small amount of liquid would be present at 630°C and the lower value is quoted at 620°C. The results, while underestimating the measured values, are still in very reasonable agreement and the temperature dependency of the conversion of Al_6Mn to α is almost exactly predicted. Furthermore, Marshall (1996) reported results for the closely related AA3104 alloy where the transition from Mg_2Si to α is observed somewhere between 350 and 400°C. Although Marshall (1996) did not provide a composition for the alloys which were used, calculations for an ideal 3104 composition, following Sigli *et al.* (1996), suggest this transition occurs between 360° and 440°C, in good agreement with observation.

In alloys such as AA3004 some of the major issues concern solidification and therefore it is interesting to look at this in detail. However, as solidification in Al alloys rarely occurs under equilibrium conditions, a more detailed examination of this issue will be found in the next chapter.

10.4.3 A versatile corrosion-resistant duplex stainless steel (SAF2205)

Duplex stainless steels are a highly formable, strong, yet highly corrosion-resistant series of alloys. The 'ideal' duplex structure is aimed to be a 50/50 mixture of austenite (γ) and ferrite (α). The microstructure can be manipulated by thermo-mechanical processing to produce an alloy with high strength. They also have a high Pitting Resistance Equivalent (PRE), where PRE can be related to the levels of Cr, Mo, W and N by the empirical formula (Hertzman 1995)

$$\text{PRE} = \text{wt\%Cr} + 3.3(\text{wt\%Mo} + \text{wt\%W}) + 16\text{wt\%N}.$$

A popular alloy of this type is SAF 2205. The alloy is predominantly an Fe–Cr–Ni alloy with significant additions of Mo, Mn, Si, C and N. The composition may typically be Fe–22Cr–5.5Ni–3Mo–1.7Mn–0.4Si–0.14N–0.024C (in wt%). Figure 10.29 shows an isothermal section for Fe–Cr–Ni at 1000°C and Fig. 10.30 shows a phase% vs temperature plot for a Fe–22Cr–5.5Ni alloy. It has a narrow liquid+solid region and it is already duplex below 1216°C, reaching a 50/50 $\gamma + \alpha$ mixture at 1015°C, close to the final annealing temperature of the full composition alloy. The σ phase forms below 730°C at the expense of α, but this is low compared to the temperature where it is observed in real SAF2205 (Thorvaldsson *et al.* 1985). The PRE number for this ternary alloy is only 22 and values around 30–40 are necessary for adequate corrosion resistance.

The addition of 3%Mo improves its pitting resistance equivalent (PRE) but causes substantial changes (Fig. 10.31). The level of austenite is substantially decreased, only forming below 1134°C and never reaching more than 40% in the

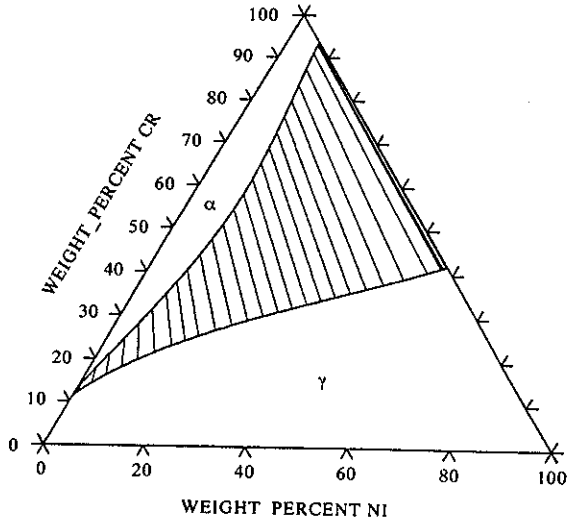

Figure 10.29 Calculated isothermal section for Fe–Cr–Ni at 1000°C.

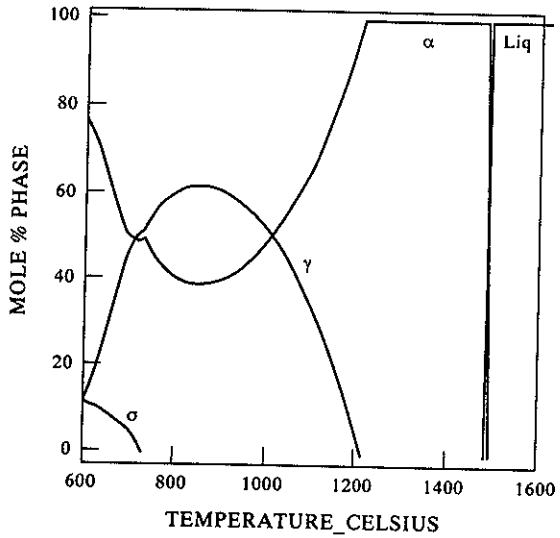

Figure 10.30 Calculated mole % phase vs temperature plots for a Fe–22Cr–5.5Ni alloy.

References are listed on pp. 402–408.

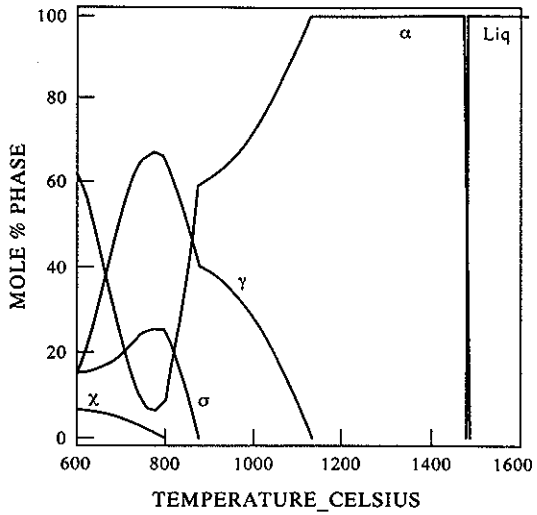

Figure 10.31 Calculated mole % phase vs temperature plots for a Fe–22Cr–5.5Ni–3Mo alloy.

duplex region. The stability of σ is markedly increased: it now forms below 875°C and some χ forms below 800°C. Both σ and χ are actually seen in SAF2205. Figure 10.32 shows an isothermal section for Fe–Cr–Mo which shows the expansive region of σ and the formation of a ternary χ phase.

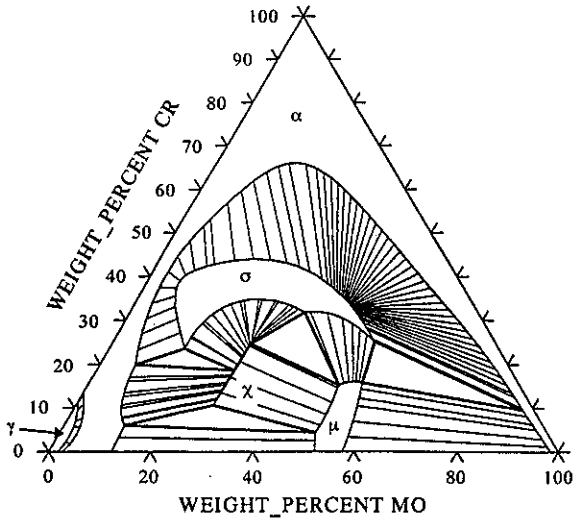

Figure 10.32 Calculated isothermal section for Fe–Cr–Mo at 1000°C.

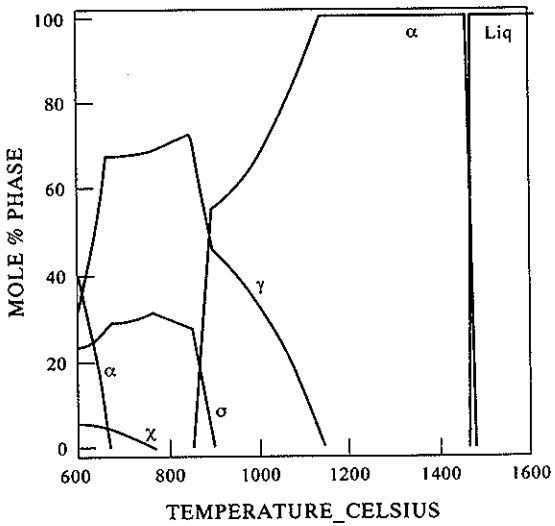

Figure 10.33 Calculated mole % phase vs temperature plots for a Fe–22Cr–5.5Ni–3Mo–1.7Mn alloy.

The addition of 1.7%Mn does not make such a large difference as the Mo addition (Fig. 10.33). It is, however, noticeable that all of the α has disappeared between 670–850°C by the reaction to form $(\gamma + \sigma)$. This is because Mn is both a γ stabiliser and it enhances the formation of σ which competes with α for α-stabilising elements such as Cr and Mo.

The addition of 0.4wt%Si does not alter the general behaviour of the alloy significantly (Fig. 10.34). It is known that a ternary σ phase forms in Fe–Cr–Si but Si is also a powerful α stabiliser. It is noticeable that there has been sufficient α stabilisation to delay the onset of the $\alpha \rightarrow (\gamma + \sigma)$ transformation and α is stable to lower temperatures than previously but, in the end, the level of addition of Si is insufficient to make significant changes.

The next major changes occur with addition of N which substantially stabilises γ (Fig. 10.35). The alloy is now close to its final composition and it can be seen that the N has stabilised γ sufficiently such that it becomes the predominant phase below 1050°C while the formation of σ and χ is relatively unchanged. A new phase is now observed, M_2N, based on Cr_2N. This is an important phase as it can cause sensitisation to corrosion resistance. In SAF2205 its temperature of formation is close to that of σ. The addition of C additionally causes the formation of $M_{23}C_6$ below 900°C (Fig. 10.36) and slightly lowers the solidus.

The final predicted behaviour for SAF2205 is close to that found in practice. The amount of γ in the alloy as a function of temperature is in excellent agreement with experimental results (Hayes 1985) and the behaviour of the minor phases is also

References are listed on pp. 402–408.

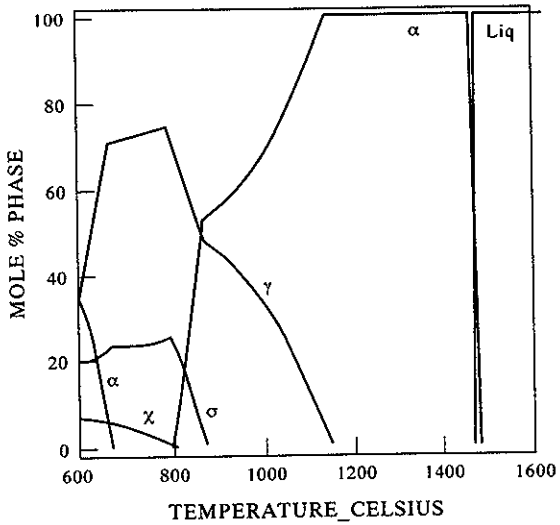

Figure 10.34 Calculated mole % phase vs temperature plots for a Fe–22Cr–5.5Ni–3Mo–1.7Mn–0.4Si alloy.

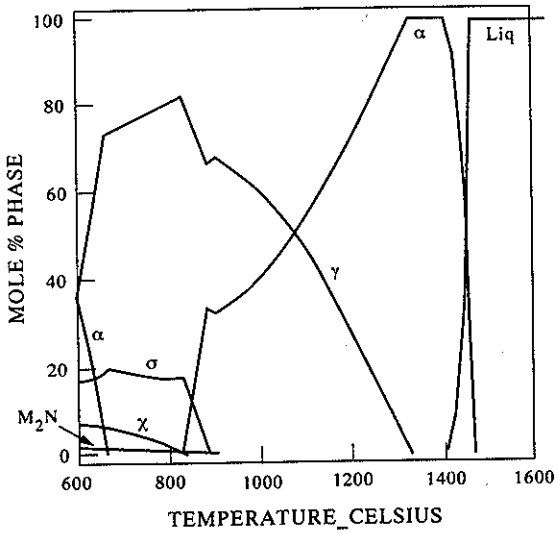

Figure 10.35 Calculated mole % phase vs temperature plots for a Fe–22Cr–5.5Ni–3Mo–1.7Mn–0.4Si–0.14N alloy.

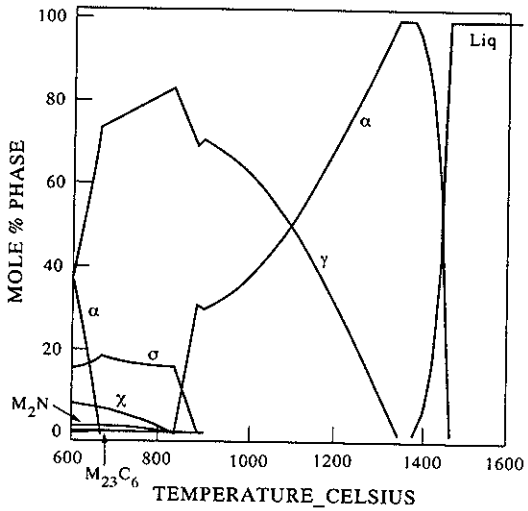

Figure 10.36 Calculated mole % phase vs temperature plots for a SAF2205 alloy with composition Fe–22Cr–5.5Ni–3Mo–1.7Mn–0.4Si–0.14N–0.24C.

well predicted. The temperature of σ and M_2N formation is close to that observed in practice and the $M_{23}C_6$ and χ phases are predicted to form as observed (Thorvaldsson *et al.* 1985). The behaviour of the χ phase is interesting as it is commonly seen as one of the first minor phases to form in practice. Thorvaldsson *et al.* (1985) showed that in SAF2205 the sequence of phase formation at 850°C would be χ followed by σ, with σ finally being the stable phase and χ disappearing after long anneals. The predicted solvus temperature for χ is close to that of σ but at 850°C it is not yet stable when σ forms. This would be quite consistent with the observed behaviour of SAF2205.

10.5. QUANTITATIVE VERIFICATION OF CALCULATED EQUILIBRIA IN MULTI-COMPONENT ALLOYS

This section will give examples of how CALPHAD calculations have been used for materials which are in practical use and is concerned with calculations of critical temperatures and the amount and composition of phases in duplex and multi-phase types of alloy. These cases provide an excellent opportunity to compare predicted calculations of phase equilibria against an extensive literature of experimental measurements. This can be used to show that the CALPHAD route provides results whose accuracy lies close to what would be expected from experimental measurements. The ability to statistically validate databases is a key factor in seeing the CALPHAD methodology become increasingly used in practical applications.

References are listed on pp. 402–408.

10.5.1 Calculations of critical temperatures

In terms of practical use, one of the most important features of phase equilibria can often be the effect of composition on some critical temperature. This can be a liquidus or solidus or a solid-state transformation temperature, such as the β-transus temperature, (T^β), in a Ti alloy. The solidus value can be critical, as solution heat-treatment windows may be limited by incipient melting. In some materials a solid-state transformation temperature may be of prime importance. For example, in Ti alloys it may be specified that thermomechanical processing is performed at some well-defined temperature below the β-transus temperature. The CALPHAD route provides a method where such temperatures can be quickly and reliably calculated.

10.5.1.1 Steels. One of the most striking successes of the CALPHAD technique has been in the highly accurate calculation of liquidus and solidus temperatures. Because of their inherent importance in material processing, there are numerous reported measurements of these values, which can be used to judge how well CALPHAD calculations perform in practice. For example, detailed measurements of liquidus and solidus values for steels of all types have been made by Jernkontoret (1977). The values were obtained on cooling at three different cooling rates, 0.5, 1 and 5°C sec^{-1}. The effect of cooling rate is seen to be marginal on the liquidus but could be profound on the solidus due to the effects of non-equilibrium segregation during the liquid→solid transformation. Calculations for the liquidus and solidus were made for these alloys using the Fe-DATA database (Saunders and Sundman 1996) and compared with the results obtained at the lowest cooling rate. Figure 10.37 shows the results of this comparison and the accuracy of the predictions is impressive, particularly for the liquidus values which exhibit an average deviation from experiment ($\bar{d}$) of only 6°C. It is also pleasing to note how well the solidus values are predicted with an average deviation of just under 10°C. Three solidus values are not matched so well and are highlighted. In these alloys low-melting eutectics were observed, but not predicted, and it is uncertain if the difference is due to an inherent inaccuracy in the prediction or to the persistence of non-equilibrium segregation during solidification.

10.5.1.2 Ti alloys. In Ti alloys there are numerous measurements of the T^β as this is a very critical temperature for these alloys. Figure 10.38 shows the comparison between predicted and measured values for Ti alloys of all types, ranging from β-type alloys such as Ti–10V–2Al–3Fe through to the α types such as IMI834. The results exhibit an average deviation from experiment of less than 15°C which is very good for the measurements of a solid-state transformation such as T^β.

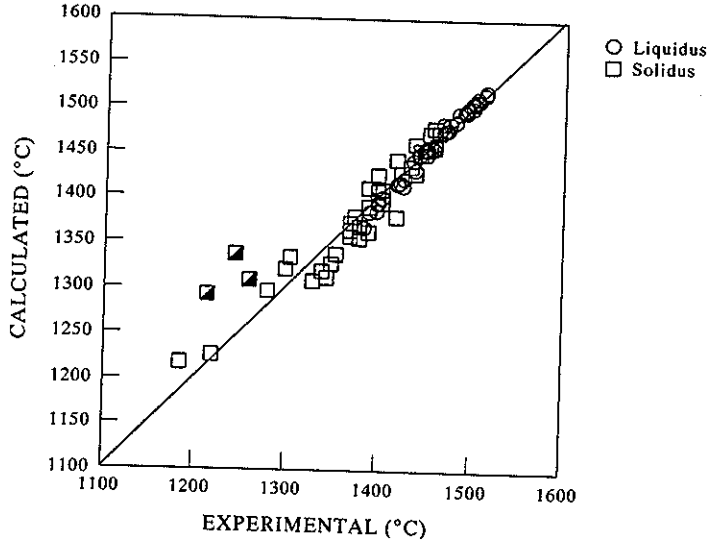

Figure 10.37 Comparison between calculated and experimental (Jernkonteret 1977) solidus and liquidus values of a range of steels.

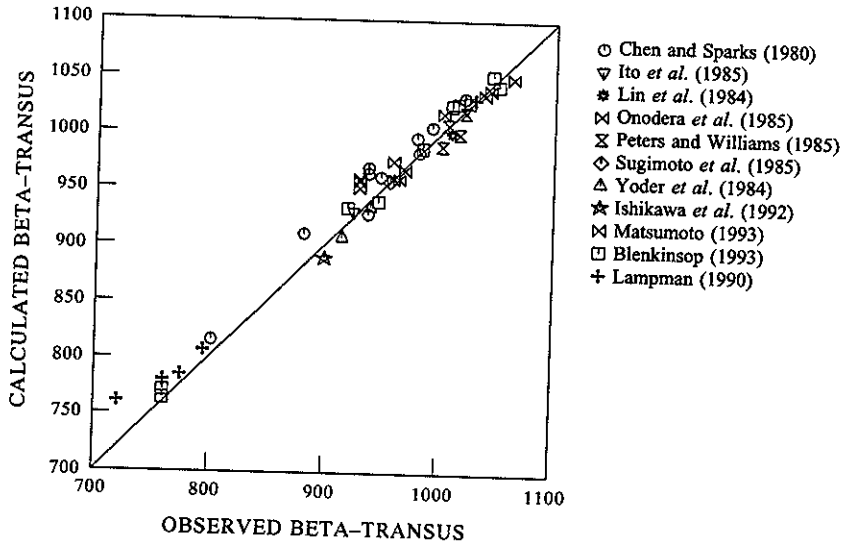

Figure 10.38 Comparison between calculated and experimental β-transus temperatures in Ti–alloys (from Saunders 1996a).

References are listed on pp. 402–408.

10.5.1.3 Ni-based superalloys. In Ni-based superalloys, containing high volumes of γ', the temperature window where an alloy can be heat treated in the fully γ state is a critical feature both in alloy design and practical usage. This heat treatment window is controlled both by γ'_s and the solidus and there have therefore been numerous experimental measurements of these properties. A further key experimental feature for cast alloys is the liquidus and, similarly, numerous measurements have also been made for this temperature. Figure 10.39 shows a comparison plot for γ'_s, liquidus and solidus for wide variety of Ni-base superalloys and average deviations from experiment are typically the same as for steels and Ti alloys, with $\bar{d}$ for liquidus and solidus being 6°C and 10°C respectively while $\bar{d}$ for the γ'_s is less than 15°C.

10.5.2 Calculations for duplex and multi-phase materials

10.5.2.1 Duplex stainless steels. Duplex stainless steels have provided a fruitful area for CALPHAD calculations and have been an example of where high levels of success have been achieved for practical materials. An early study (Hayes 1985) was able to demonstrate that reasonable predictions for amounts of austenite could be obtained for a variety of different duplex stainless steels, demonstrating the

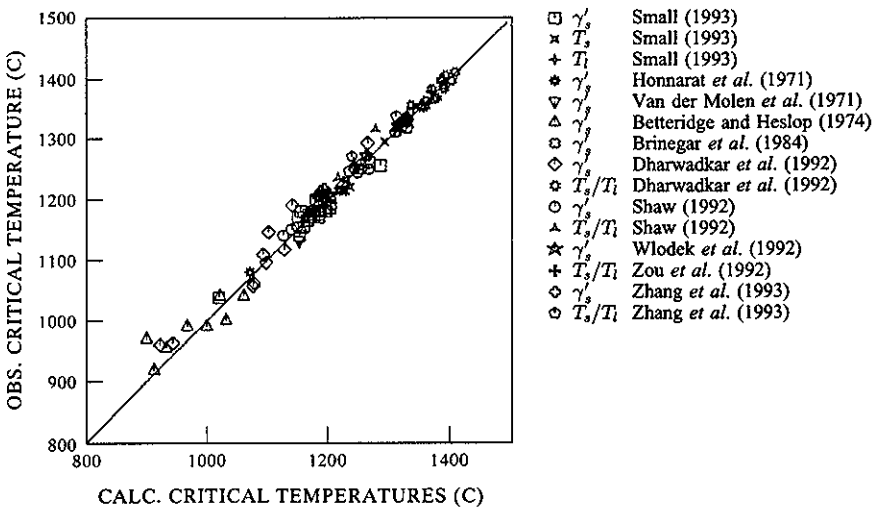

Figure 10.39 Comparison between calculated and experimental critical temperatures for Ni-based superalloys (from Saunders 1996c).

general applicability of CALPHAD calculations to these materials. The later work of Longbottom and Hayes (1994) shows how a combination of CALPHAD calculation and experiment can provide accurate formulae for the variation in austenite and ferrite as a function of composition and heat-treatment temperature in Zeron 100 stainless steels. These formulae can then be used during production of the material to help define temperatures for thermomechanical processing. The steel database (TCFe) developed at KTH has been used in a number of publications, notably by Nilsson (1992) and Hertzman (1995).

More recently, Fe-DATA (Saunders and Sundman 1996) was used in calculations for a wide variety of duplex stainless steels, and detailed comparisons were made for amounts of austenite, as a function of temperature, and the partition coefficients of various elements in austenite and ferrite. The results of these comparisons are shown in Figs 10.40 and 10.41. In Fig. 10.40, experimental results which have been given as volume fractions have been compared with mole% predictions, which is reasonable as molar volumes of the two phases are very similar. $\bar{d}$ for the amount of austenite is less than 4%, of the same order as would be expected for experimental accuracy, and the comparison of elemental partition coefficients is good. C and N levels, which are difficult to measure in practice, are automatically calculated. Where such measurements have been made the comparison is good and the advantage of using a calculation route is further emphasised.

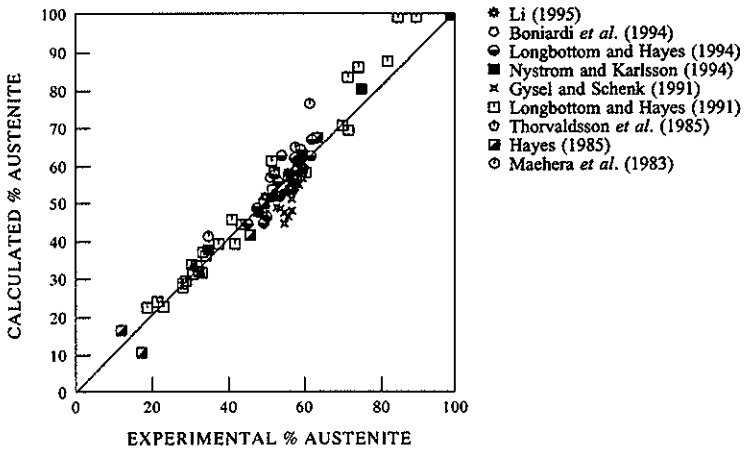

Figure 10.40 Comparison between calculated and experimentally observed % of austenite in duplex stainless steels. (Data from Longbottom and Hayes (1991) represent dual phase steels.).

References are listed on pp. 402–408.

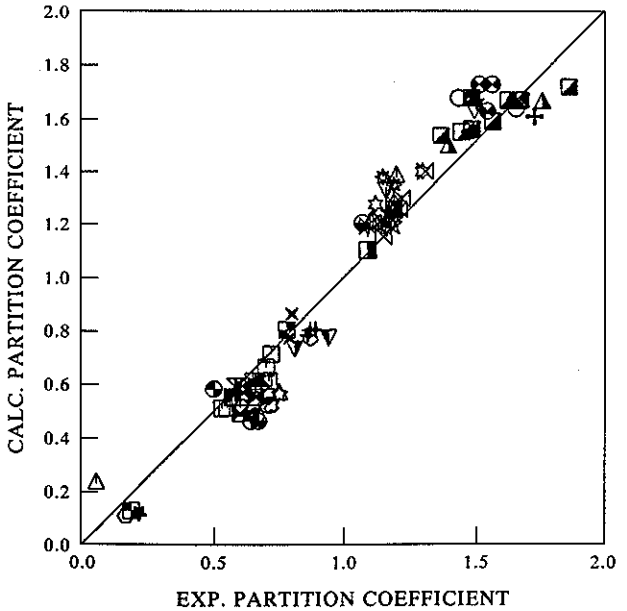

Figure 10.41 Comparison between calculated and experimentally observed partition coefficients between austenite and ferrite in duplex stainless steels.

10.5.2.2 Ti alloys. Duplex microstructures are usually formed in Ti alloys which are classed using the level of α-Ti or β-Ti in the alloy. There are a few fully α and β alloys but most are duplex in nature. Much work has been done in measuring T^{β} but fewer results are available in the open literature for the variation of volume fraction and composition of α and β. Fewer experiments are therefore available for comparison purposes. Figures 10.42(a–c) show calculated phase% vs temperature plots for three types of commercial alloys, an α-type, IMI834, an (α/β)-type, SP 700 and a β-type Ti–10V–2Al–3Fe. The agreement is very satisfactory.

10.5.2.3 High-speed steels. High-speed steels are alloys with high C levels and containing refractory metals such as Cr, Mo, V and W. They subsequently contain high levels of various carbides, typically between 5 and 15 vol%, with some alloys having more than 20 vol% (Riedl *et al.* 1987, Hoyle 1988, Wisell 1991, Rong *et al.* 1992). They are useful practical alloys for cutting tools where their wear resistance, toughness and resistance to tempering during machining is controlled by the types, amounts and shapes of the various primary carbides M_6C, M_2C and MC. The composition of the steel controls the amounts and types of the various carbides and, therefore, knowledge of phase equilibria in these alloys is important. Detailed work has been done by Wisell (1991) characterising the various carbides in tool steels. Fifty-six alloys were prepared and compositions of the carbides measured by microprobe analysis. Calculations have been made for all alloys and comparisons with the composition of the various M_6C, M_2C and MC carbides are shown in Figs. 10.43(a–c).

10.5.2.4 Ni-based superalloys. In Ni-based superalloys considerable work has been done on the determination of γ/γ' equilibria and a substantial literature exists by which to compare CALPHAD calculations with experimental results. Figure 10.44 shows a comparison plot for γ' amounts in a wide variety of superalloys, ranging from low γ' types such as Waspaloy through highly alloyed types such as IN939 to single crystal alloys such as SRR99. The accuracy is similar to that for the duplex steels, with $\bar{d}$ of the order of 4%. As lattice mismatches are so small, mole% values give almost identical values to vol% and figures 10.45(a–e) show some of the comparisons for the composition of γ and γ' where the high standard of results is maintained. Where experimental results have been quoted in wt% they have been converted to at% to allow for consistency of comparison. The average difference for elements such as Al, Co and Cr is close to 1at% while for Mo, Ta, Ti and W this value is close to 0.5at%. Too few experimental values for Hf and Nb were found to be statistically meaningful but where possible these were compared and results for average differences were found to be slightly better than obtained for Mo, Ta, Ti and W.

References are listed on pp. 402–408.

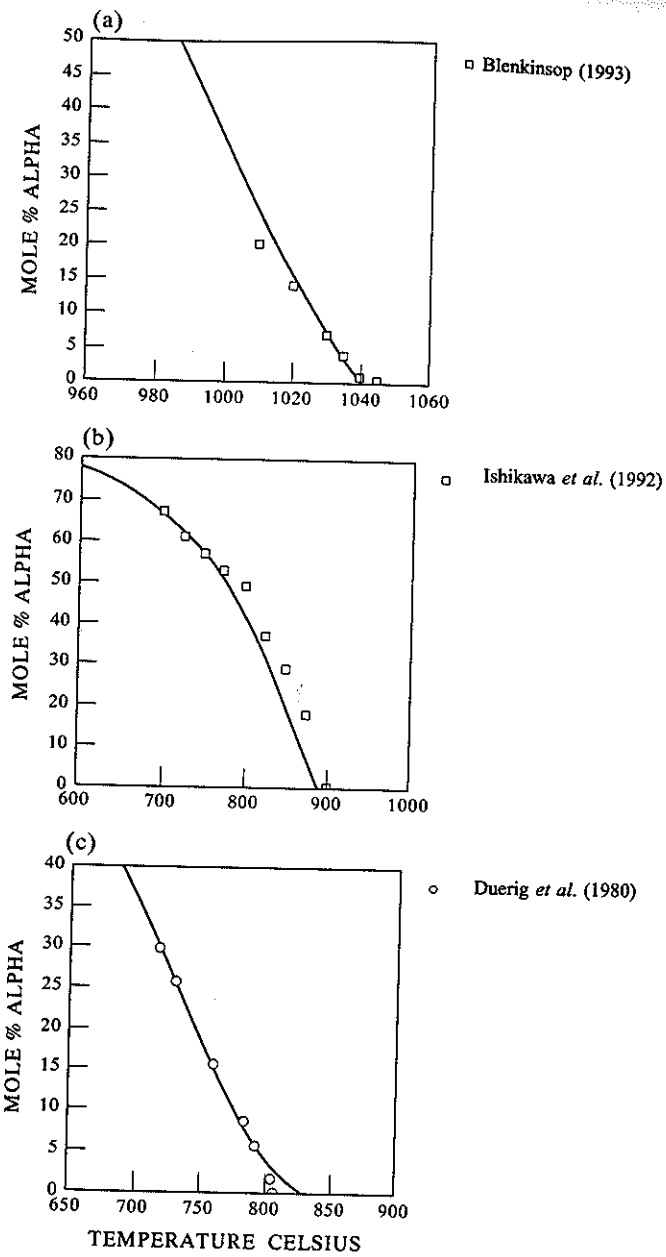

Figure 10.42 Calculated mole % phase vs temperature plots for three types of commercial alloys: (a) an α-type, IMI 834, (b) an (α/β)-type, SP 700 and (c) a β-type Ti–10V–2Al–3Fe (from Saunders 1996a).

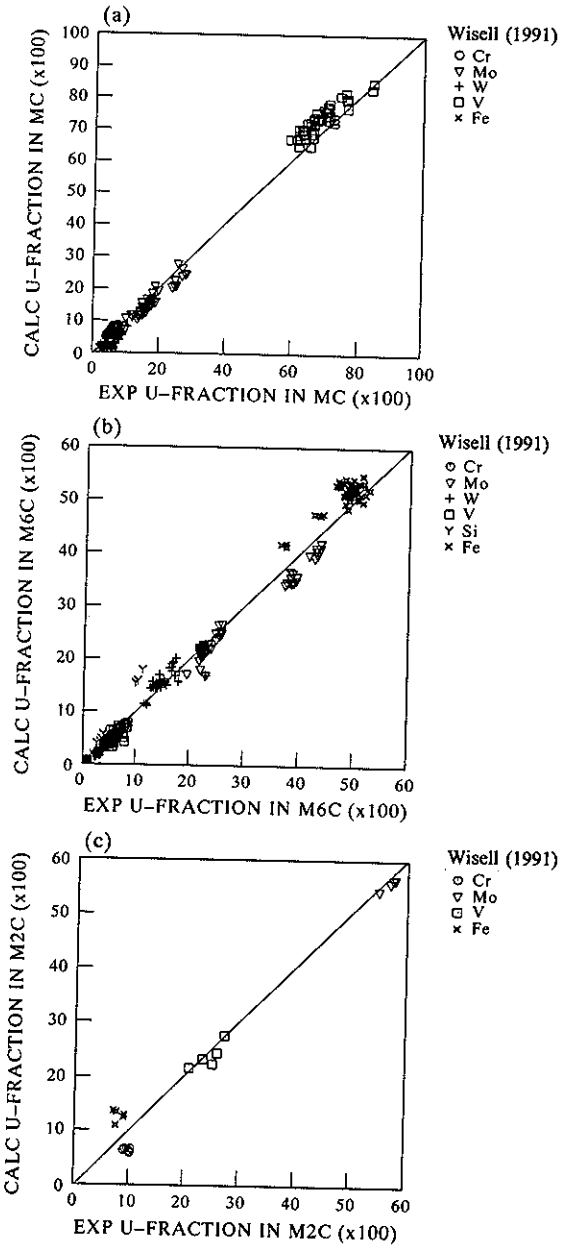

Figure 10.43 Comparison between calculated and experimental values (Wisell 1991) for the concen-tration of Cr, Mo, W, V and Fe in (a) the MC, (b) the M_6C and (c) M_2C phases of high-speed steels.

References are listed on pp. 402–408.

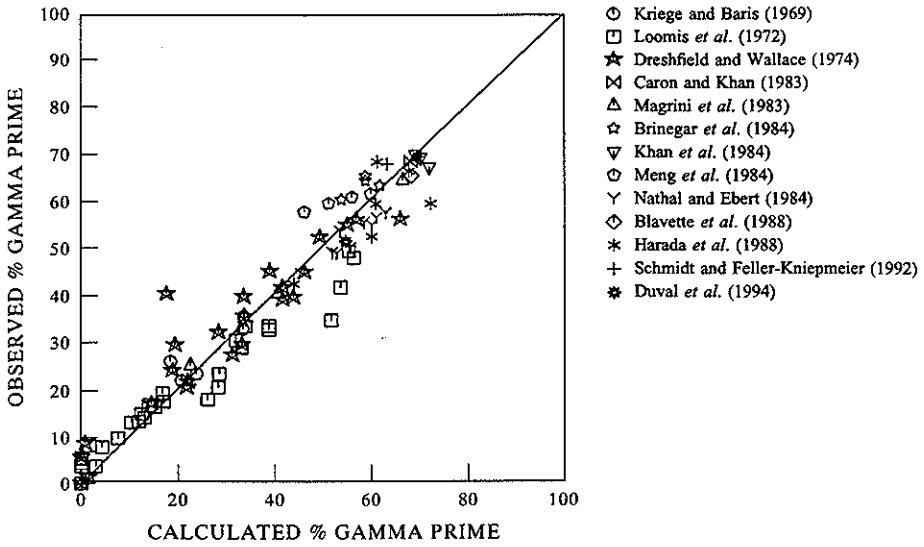

Figure 10.44 Comparison between observed and calculated amounts of γ' in Ni-based superalloys (from Saunders 1996c).

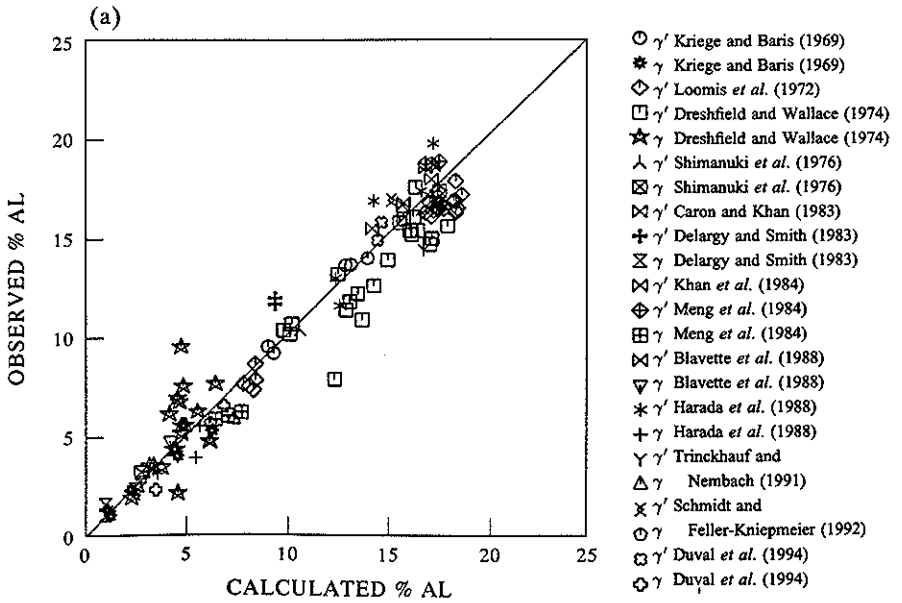

Figure 10.45 Comparison between calculated and observed compositions of γ and γ' in Ni-based superalloys: (a) Al, (b) Co, (c) Cr, (d) Mo and (e) W. (at %) (from Saunders 1996c)

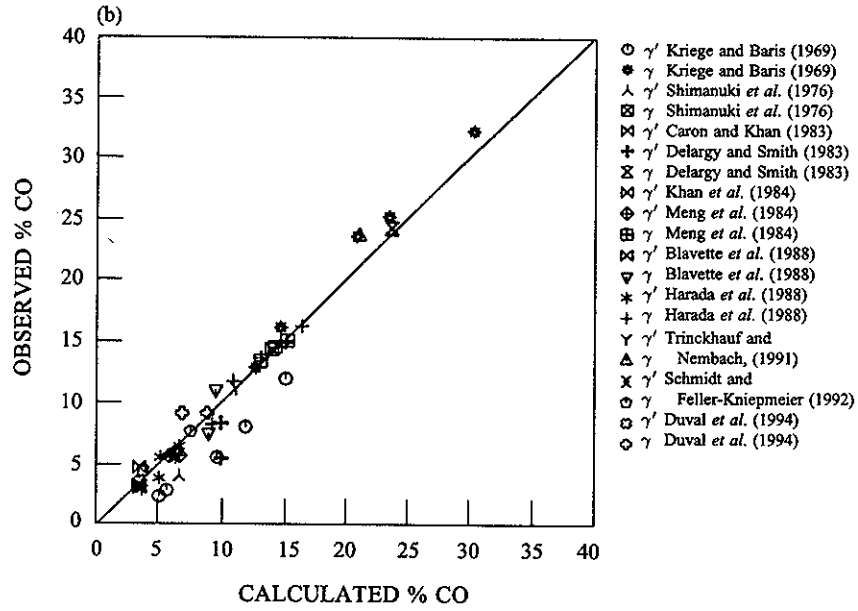

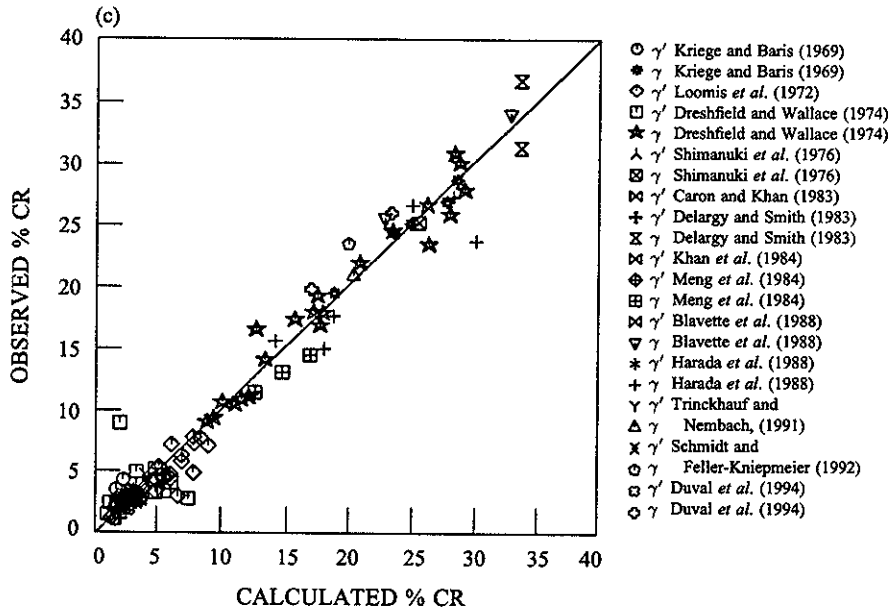

Figure 10.45 (b) and (c).

References are listed on pp. 402–408.

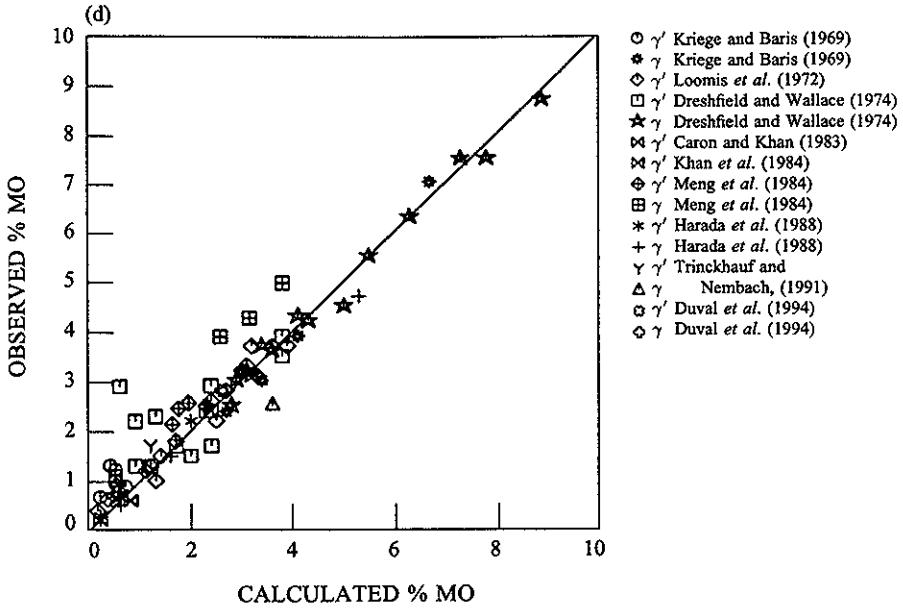

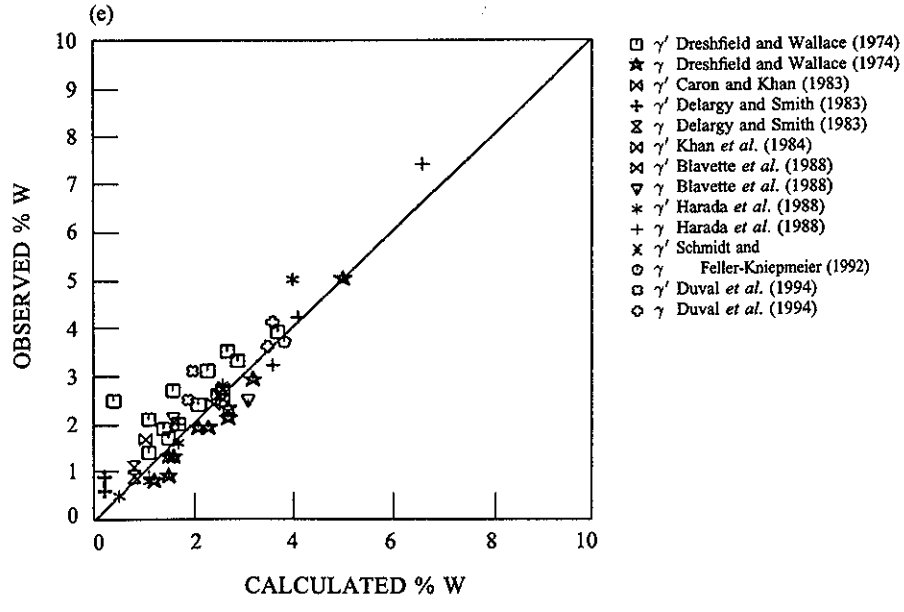

Figure 10.45 (d) and (e).

10.5.3 Summary

It is clear from the results shown in this section that the CALPHAD route is providing predictions whose accuracy lies close to that expected from experimental measurement. This has significant consequences when considering CALPHAD methods in both alloy design and general everyday usage as *the combination of a high quality, assessed database and suitable software package can, for a wide range of practical purposes, be considered as an information source which can legitimately replace experimental measurement.* The next sections discuss more complex types of calculations which are geared to specific, practical problems.

10.6. SELECTED EXAMPLES

10.6.1 Formation of deleterious phases

Formation of secondary phases is a feature of many materials and, in the context used here, is defined as the formation of phases other than the primary hardening phases or the predominant phases in duplex alloys. Embrittling phases can be carbides, borides, topologically close-packed (TCP) phases such as σ or μ, or 'insoluble' compounds such as Al_7Cu_2Fe in Al alloys. They can also be beneficial, providing secondary hardening reactions as for example in the low-temperature precipitation of η phase in the γ'-hardened alloy IN939 (Delargy and Smith 1983). But, more often, they produce a degradation in mechanical properties as is found with σ formation in stainless steels. The understanding of the formation of these phases is therefore critical in material design and processing. For Ni-based superalloys, the formation of σ and related phases has concerned alloy designers for many years. They are major materials in aerospace gas turbine engines where failure of critical components can have catastrophic consequences. The next two sub-sections will therefore show examples of how CALPHAD methods can be used to understand and help control TCP phases.

10.6.1.1 σ-Phase Formation in Ni-based Superalloys. The concept of 'σ-safety' has been one of the most important design criteria in the design of superalloys (Sims 1987), and in the past the most usual method of predicting this was by techniques such as PHACOMP which rely on the concept of an average electron hole number, $\bar{N}_v$, made up of a weighted average of $\bar{N}_v$ values for the various elements. In itself the concept behind PHACOMP is simple and it is easy to use, but there are a number of questions concerning its use and theoretical justification. For example, the values of N_v used to calculate N_v are usually empirically adjusted to fit experience and the model fails to explain why σ appears in the Ni–Cr–Mo ternary but is not observed in binary Ni–Cr or Ni–Mo. Furthermore, although it supposedly correlates with the phase boundary of γ and σ, it gives no information on the temperature range where σ may be stable, nor does it provide any information on the interaction of this boundary with the γ/μ or γ/Laves boundaries.

Using the CALPHAD route an actual σ-solvus temperature can now be calculated which defines the temperature below which σ will form and can be unambiguously used to help define 'σ-safety'. A good example of this concept is in Udimet® 720 (U720) whose composition is given below (Keefe *et al.* 1992).

	C	Cr	Co	Mo	W	Ti	Al	B	Zr
U720	0.035	18.0	14.7	3.0	1.25	5.0	2.5	0.033	0.03
U720LI	0.01	16.0	14.7	3.0	1.25	5.0	2.5	0.015	0.03

This alloy was first used in land-based gas turbine engines and for long-term use at up to 900°C (Keefe *et al.* 1992), but its excellent all-round properties suggested that it could also be used as an aerospace disc alloy. Unfortunately, while long-term exposure at high temperatures produced only minor susceptibility to σ, its use at 750°C quickly led to large amounts of σ being formed (Keefe *et al.* 1992). Clearly the alloy was either close to, or just below, its σ-solvus at the higher temperature and it was found necessary to reduce Cr levels to destabilise σ at lower temperatures. This led to the development of U720LI with 2wt% less Cr than for U720. C and B levels were also lowered to reduce formation of borides and carbides which acted as nucleation sites for σ formation.

Figure 10.46 shows a calculated phase % vs temperature plot for U720 and it can be seen that its σ-solvus is indeed close to 900°C and at 750°C the alloy would

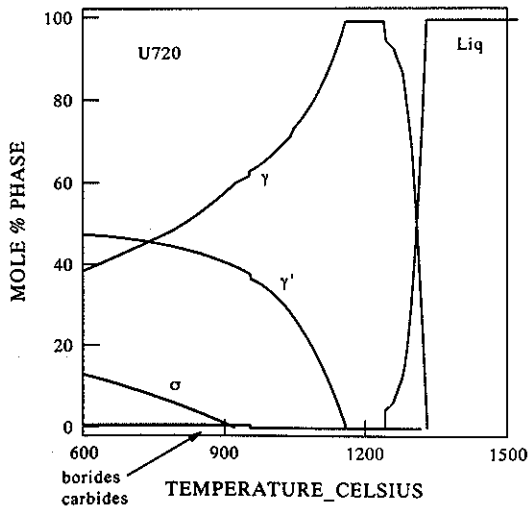

Figure 10.46 Calculated mole % phase vs temperature plot for U720 (from Saunders 1996c).

References are listed on pp. 402–408.